Title
Immune Activated Pathways in Huntington's Disease

Author
Larkin, Paul

Publication Date
2012

Peer reviewed|Thesis/dissertation

Immune Activated Pathways in Huntington's Disease

by

Paul Larkin

DISSERTATION

Submitted in partial satisfaction of the requirements for the degree of

DOCTOR OF PHILOSOPHY

in

Neuroscience

in the

GRADUATE DIVISION

of the

UNIVERSITY OF CALIFORNIA, SAN FRANCISCO

Acknowledgements

I would like to first acknowledge my thesis advisor, Paul Muchowski. His enthusiasm for science and for discussing science spurred me to come to UCSF and to join his lab, and that contagious enthusiasm has helped me sustain my efforts though the ups and downs of grad school.

My thesis committee – Lennart Mucke, Erik Ullian, Tony DeFranco and Katerina Akassoglou – stuck with me through many twists, turns and tangents and managed to offer extremely insightful comments throughout.

My lab mates in the Muchowski lab were a crucial source of all kinds of support and knowledge. Robbie Schwarcz and my collaborators in his lab, particularly Sai Kumar, were great to work with and were integral to the success my Kynurenine Pathway projects.

Through everything, my family and friends (especially my classmates) have been a constant source of advice, perspective and fun.

Thank you most of all to Maggie Carr for her love and support, and for laughing at even the wurst of my jokes.

Author Contributions

The text of Chapter 2 of this thesis has been published in *Journal of Huntington's Disease* (Larkin and Muchowski, 2012). Paul Larkin performed and analyzed all experiments described in this chapter under the supervision of Paul Muchowski, the senior author on the publication. Paul Larkin and Paul Muchowski co-wrote the paper.

The text of Chapter 3 of this thesis is a preliminary version of a manuscript that will be submitted to the Journal of Biological Chemistry. Paul Larkin collected all samples used in these experiments. TDO deficient mice were provided by Hiroshi Funakoshi and Toshikazu Nakamura, the fourth and fifth authors on the manuscript. Paul Larkin and Sai Kumar, the second author on the manuscript, together collected all the enzyme activity and HPLC based data except KAT I and KAT II activity in brain and 3HAO activity in liver, which was collected by Sai Kumar. Francesca Notarangelo, the third author on the manuscript, collected all GC/MS based data. Data on biogenic amines were obtained by Raymond Johnson at the Vanderbilt Neurochemistry Core. Paul Larkin collected all qPCR based data and all data on NAD levels. Robert Schwarcz and Paul Muchowski, the senior authors on the manuscript, supervised all research. Paul Larkin wrote the manuscript under the supervision of Paul Muchowski.

Abstract

Many studies of immune responses in neurodegeneration assert that neuroinflammation is a double edged sword – i.e. some aspects of an immune response are beneficial while others are detrimental. In this thesis we investigated two enzymatic cascades that are activated in response to inflammatory stimuli and that we hypothesized were relevant for Huntington's Disease (HD).

In Chapter 2 we explored the role of the complement cascade in the R6/2 mouse model of HD. The complement cascade is a well characterized immune response mechanism and it is activated in brains of HD patients. Surprisingly, we found that this upregulation of the complement cascade is not mirrored in the R6/2 mouse model of HD, and that genetic deficiency in complement component C3 does not alter disease progression in these mice. This illustrates that normal complement cascade activity is not necessary for disease progression in R6/2 mice, with the caveat that complement activation in HD patients is not faithfully reproduced in this mouse model of HD.

In Chapter 3 we turned our attention to a pathway known to be relevant in HD, the Kynurenine Pathway. Here, instead of seeking a link between the pathway and HD, we sought to understand how two types of Kynurenine Pathway activity, basal and immune stimulated, are controlled. We employed mice genetically deficient in either tryptophan 2,3-dioxygenase (TDO) or indoleamine 2,3-dioxygenase (IDO) because these two enzymes can catalyze the rate-limiting step of the Kynurenine Pathway. We evaluated the contribution

of each enzyme to basal and immune stimulated production of several Kynurenine Pathway metabolites that play a role in a variety of highly prevalent diseases, including HD. TDO deficient mice show evidence of several compensatory changes in basal Kynurenine Pathway metabolism. These changes suggest the existence of important unknown mechanisms that regulate basal Kynurenine Pathway metabolism. In contrast, IDO deficient mice appear to be a useful tool for cleanly blocking inflammation induced increases in brain Kynurenine Pathway metabolites without altering basal Kynurenine Pathway metabolism. Both of these results have important implications for development of therapeutics targeting the Kynurenine Pathway.

Table of Contents

List of Tables and Figures

Chapter 1

Chapter 2

Chapter 3

Chapter 1

Introduction

Pro-inflammatory activation of the immune system is a feature of many neurodegenerative diseases. However, like all inflammatory responses, inflammation during neurodegeneration is a complex and multifaceted process that likely includes both beneficial and detrimental aspects. In this thesis, I describe my experiments aimed at exploring two aspects of the inflammatory response that may contribute to the neurodegeneration that occurs during Huntington's Disease (HD). In many neurodegenerative diseases inflammation only occurs at late stages of disease progression. In contrast, HD is a particularly appropriate setting in which to study inflammation because in HD there are signs of inflammation long before other overt symptoms appear. In Chapter 2 I will describe my experiments on the role of the complement cascade in HD. Regulation and function of the complement cascade have been well described in the context of the immune system, but it is only recently that several studies have shown that the complement cascade is important in the brain as well. In Chapter 3 I will describe my experiments on mechanisms by which the immune system regulates Kynurenine Pathway function in the brain. Many studies have suggested that the Kynurenine Pathway is important in HD, so I sought to elucidate the major determinants of Kynurenine Pathway regulation in an attempt to identify new therapeutic targets for HD.

Huntington's Disease

Huntington's disease (HD) is an adult onset neurodegenerative disease that is inherited in an autosomal dominant fashion. The disease is caused by an increase in the number of CAG repeats in the *IT-15* gene which translates to an increase in the length of a polyglutamine repeat in the protein huntingtin. Individuals who posses a copy of the gene with more than 37 CAG repeats will get HD, while individuals with fewer than 34 CAG repeats are unaffected [1]. The expanded polyglutamine region of the protein can aggregate *in vitro,* and *in vivo* it contributes to the formation of intracellular inclusion bodies [2,3]. These inclusion bodies are aggregates of both the mutated huntingtin protein and many other diverse cellular proteins. Inclusion bodies may be pathogenic due to their role in sequestering these other cellular proteins. However, they can also serve a protective function, perhaps because they sequester the harmful mutant huntingtin protein [4]. In addition to a toxic gain of function, mutant huntingtin may contribute to toxicity by inhibiting some of the functions of normal huntingtin [5]. Downstream of mutant huntingtin, many mechanisms have been hypothesized to play a role in the progression of HD [6]. Among these, two prominent hypotheses are 1) that reactive oxygen species accumulate and cause widespread cellular damage and 2) that excessive stimulation of NMDA receptors on neurons leads to excitotoxic neuronal death. These mechanisms are particularly relevant for this thesis as many studies indicate that the Kynurenine Pathway can contribute to both generation of reactive oxygen species and NMDA receptor activation.

The neuronal death that is a hallmark of HD occurs first in the medium spiny neurons of the striatum, despite the fact that mutant huntingtin is expressed ubiquitously throughout the body [7]. Though medium spiny neurons are selectively vulnerable to mutant huntingtin expression, the disease eventually leads to neurodegeneration throughout the brain. In addition to frank loss of neurons, HD patients and mouse models of HD have significant dendritic spine and synapse loss, suggesting that spine or synaptic dysfunction may play an important role in disease progression [8]. This is particularly relevant for this thesis as recent research has shown that complement plays a role in synapse remodeling.

The medium spiny neurons that degenerate first in HD are involved in inhibition of movement, and their degeneration leads to the most visible symptom of HD: progressive loss of motor control resulting in chorea, or involuntary dance-like movements. These idiosyncratic motor behaviors are the easiest symptoms to identify, but the disease also leads to cognitive and emotional symptoms and ultimately death. Despite decades of research, current treatments are largely ineffective at altering disease progression.

Role of the Immune System in Huntington's Disease

In addition to neuronal dysfunction, HD patients also have prominent alterations of the immune system. Expression of mutant huntingtin can be observed in cells of the immune system including lymphocytes, fibroblasts, erythrocytes and microglia – the immune cells of the brain. In cells outside of the

brain, this expression of mutant huntingtin both compromises function [9,10] and leads to altered production of immune system signaling molecules such as cytokines [11–13]. In HD patients, some cytokines are present in the blood at abnormally high levels many years before onset of other disease symptoms [11]. These changes can serve as biomarkers of HD and some of them may also contribute to disease progression. For example, work in our lab has shown that inhibition of peripheral immune signaling mediated by either endocannabinoid or IL-6 signaling can alter disease progression in a mouse model of HD [14].

Alterations of the immune system inside the brain may also contribute to HD progression. Many chronic neurodegenerative diseases, including HD, are associated with chronic neuroinflammation that includes activation of microglia and elevated brain levels of immune system signaling molecules including cytokines and chemokines [15,16]. In HD specifically, microglial cells are activated significantly before onset of other disease symptoms and their activation progresses with the disease. In mouse models of HD, the morphology of microglia is altered early in disease and dystrophic microglia persist throughout disease progression [17,18]. These morphological changes appear to correlate with functional alterations as microglia expressing mutant huntingtin have impaired responses to chemotactic stimuli *in vitro* and laser induced injury *in vivo* [10]. Longitudinal imaging of microglial activation in human HD patients, using a PET ligand that binds to activated microglia, shows that microglial activation occurs in presymptomatic patients carrying the disease causing gene [19,20]. Further, the degree of microglial activation correlates with disease

severity [21]. The fact that microglia are activated before symptom onset is significant because it implies that microglial activation is not simply a response to degeneration, but may instead be a driving force. Given that microglia are thought to play a role in the maintenance of a healthy synaptic environment [22–24], dysfunctional microglia may contribute to the synaptic dysfunction that also occurs early in HD.

Role of the Complement Cascade in Huntington's Disease

One aspect of neuroinflammation in HD is upregulation of several components of the complement cascade [12,16,25]. The complement cascade is an enzymatic cascade that is activated by certain types of pathogens and then contributes to proinflammatory signaling as well as pathogen destruction. The mechanisms of pathogen destruction employed by the complement cascade include binding to the pathogen and thereby signaling nearby phagocytes to engulf both the complement protein and the pathogen it has bound. The presence of many endogenous inhibitors of complement activation ensures that this is a very tightly controlled process. When complement activation is uncontrolled, complement mediated destruction is not limited to pathogens but can spread to healthy tissue nearby. Given the destructive potential of the complement cascade, it was surprising to observe increased levels of complement in HD brains and many have hypothesized that these proteins could be exacerbating neurodegeneration [26]. Interestingly, more recent work has shown that complement proteins are also upregulated in healthy brain during

development. Mice which are unable to upregulate complement during development lack normal developmental synapse elimination, suggesting that complement proteins contribute to destruction of synapses during development [27]. While this is beneficial during brain development, it may be detrimental if these same mechanisms are reactivated in an adult brain. Thus, the presence of elevated levels of complement proteins in HD brain raises the possibility that complement proteins are involved in the elimination of synapses that occurs in HD and in mouse models of HD. In Chapter 2 of this thesis we investigated this possibility using the R6/2 mouse model of HD and mice lacking a key component of the complement cascade.

Role of the Kynurenine Pathway in Huntington's Disease

In Chapter 3 of this thesis we investigated the regulation of the Kynurenine Pathway with the goal of identifying therapeutic targets for HD. The first connection between the Kynurenine Pathway and HD was established several decades ago when one of the metabolites of the Kynurenine Pathway was used to create a mouse model of HD [28]. In this model, a striatal injection of the Kynurenine Pathway metabolite quinolinic acid (QUIN) produces a lesion that appears very similar to late stage HD. The same subset of striatal neurons that are lost first in HD are also lost after a QUIN injection [29,30]. This was an early suggestion that endogenous metabolites of the Kynurenine Pathway might contribute to HD. Endogenous QUIN was the first toxic Kynurenine Pathway metabolite identified, but the pathway also produces several other bioactive

metabolites that may impact HD. Specifically, 3-hydroxy kynurenine (3HK) can potentiate QUIN neurotoxicity, while kynurenic acid (KYNA) can protect neurons from QUIN toxicity. Mechanistic studies have shown that QUIN is likely toxic to neurons because it can contribute to production of reactive oxygen species and because it is an agonist at NMDA receptors. Excessive levels of reactive oxygen species can cause widespread cellular damage, while excessive stimulation of NDMA receptors can contribute to excitotoxicity, and both of these mechanisms have been implicated in the pathogenesis of HD. 3HK likely potentiates QUIN neurotoxicity because it too is a producer of reactive oxygen species, while KYNA blocks toxicity likely because it is an antagonist at NMDA receptors. The interplay between these Kynurenine Pathway metabolites reveals the potential for alterations in regulation of the Kynurenine Pathway to impact neurodegeneration. Further correlational evidence for a role of the Kynurenine Pathway in HD comes from the observation that elevated levels of toxic QUIN and 3HK are found in brains of HD patients and mouse models of HD [31,32], while levels of the protective metabolite KYNA are decreased [33].

Recently, several studies have employed genetic animal models of HD to establish a causal link between the Kynurenine Pathway and HD progression. In a drosophila model of HD, disease progression is ameliorated in drosophila that were fed KYNA and in mutants that produce less 3HK, while disease progression is enhanced in drosophila that are fed 3HK [34,35]. In concert with these results, mouse studies have shown that a drug that increases KYNA levels in the brain can increase survival in the R6/2 mouse model of HD [36] and a KYNA analog

can increase survival in the N171-82Q mouse model of HD [37]. These findings illustrate that in these genetic *in vivo* models 3HK can exacerbate disease and KYNA can ameliorate disease, just as would be predicted from their activity in the artificial setting of QUIN induced neurotoxicity. This indicates that the Kynurenine Pathway is a promising therapeutic target in HD, but highlights the fact that successful therapeutic Kynurenine Pathway manipulations must take care to target specific metabolites.

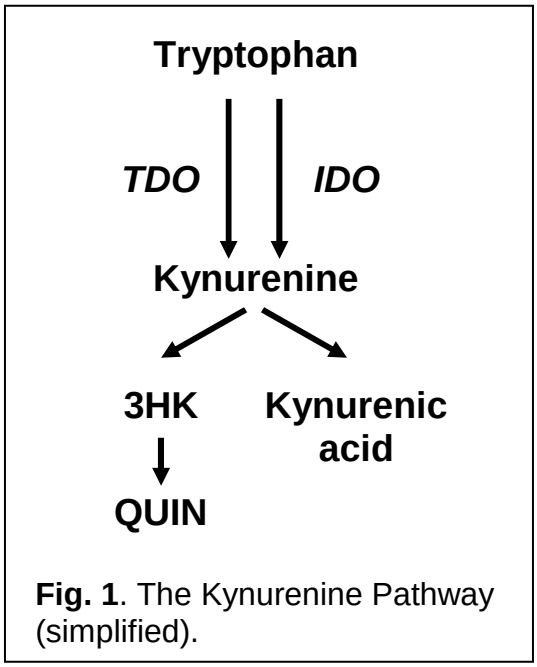

Fig. 1. The Kynurenine Pathway (simplified).

Regulation of the Kynurenine Pathway

The first and rate-limiting step of the Kynurenine Pathway is the conversion of tryptophan to kynurenine. Tryptophan is an essential amino acid that is used for protein synthesis, but the vast majority of tryptophan that is not used for protein synthesis is degraded by the Kynurenine Pathway. After

tryptophan is converted into kynurenine, the Kynurenine Pathway branches (Fig. 1). One branch uses kynurenine to produce both of the neurotoxic Kynurenine Pathway metabolites, 3HK and then QUIN, while the other branch uses kynurenine to produce the protective metabolite, KYNA. Thus, kynurenine is a pivotal molecule of the Kynurenine Pathway as it serves as a substrate for production of both neurotoxic and protective Kynurenine Pathway metabolites.

Further, kynurenine itself is important for a number of biological functions including blood pressure regulation [38] and control of T cell phenotypes [39–41]. Kynurenine's role in these processes means that pharmacological manipulation of the Kynurenine Pathway is being pursued as a possible therapy for multiple diseases. Most prominently, groundbreaking recent studies have shown that kynurenine can bias T cells towards becoming anti-inflammatory regulatory T cells (Tregs), and this process is exploited by tumors in order to evade T cell mediated destruction [42,43]. Thus, inhibitors of kynurenine production may be useful anti-cancer agents and several such drugs are in development, including one that is in a phase I/II clinical trial (clinicaltrials.gov). While the effects of these drugs may be beneficial in their target indications, their effects on downstream Kynurenine Pathway metabolites and their effects on other outcomes, including brain health, are unclear.

The two enzymes that produce kynurenine by breaking down tryptophan are indoleamine 2,3-dioxygenase (IDO) and tryptophan 2,3-dioxygenase (TDO). They catalyze the same reaction with similar kinetics, but they differ in tissue localization and regulation. TDO is constitutively expressed in the brain, liver and

a limited number of other organs, while IDO is rarely constitutively expressed but can be induced by immune stimulation in many tissues. Thus, it is logical to hypothesize that TDO is responsible for constitutive production of kynurenine and IDO is responsible for immune stimulated production of kynurenine, but these hypotheses have not been rigorously tested *in vivo*. Further, most studies of the Kynurenine Pathway assume that changes in kynurenine are mirrored by downstream Kynurenine Pathway metabolites. This too is an untested hypothesis whose validity will be very important for any attempts to manipulate specific Kynurenine Pathway metabolites. In Chapter 3 of this thesis we delve into the respective roles of these two enzymes in both naïve and immune stimulated animals. Our aim in these experiments is to explore basic Kynurenine Pathway biology so that we can better understand the effects of Kynurenine Pathway manipulation in both basal and disease states. Ultimately, we hope to determine how best to manipulate the Kynurenine Pathway for therapeutic benefit during HD and other diseases in which the pathway has been implicated.

References

[1] Andrew SE, Goldberg YP, Kremer B, Telenius H, Theilmann J, Adam S, Starr E, Squitieri F, Lin B, Kalchman MA. The relationship between trinucleotide (CAG) repeat length and clinical features of Huntington's disease. Nat. Genet. 1993;4(4):398–403.

[2] Scherzinger E, Lurz R, Turmaine M, Mangiarini L, Hollenbach B, Hasenbank R, Bates GP, Davies SW, Lehrach H, Wanker EE. Huntingtin-encoded polyglutamine expansions form amyloid-like protein aggregates in vitro and in vivo. Cell. 1997;90(3):549–58.

[3] Wanker EE. Protein aggregation in Huntington's and Parkinson's disease: implications for therapy. Mol Med Today. 2000;6(10):387–91.

[4] Arrasate M, Mitra S, Schweitzer ES, Segal MR, Finkbeiner S. Inclusion body formation reduces levels of mutant huntingtin and the risk of neuronal death. Nature. 2004;431(7010):805–10.

[5] Cattaneo E, Rigamonti D, Goffredo D, Zuccato C, Squitieri F, Sipione S. Loss of normal huntingtin function: new developments in Huntington's disease research. Trends Neurosci. 2001;24(3):182–8.

[6] Gil JM, Rego AC. Mechanisms of neurodegeneration in Huntington's disease. Eur J Neurosci. 2008;27(11):2803–20.

[7] Li SH, Schilling G, Young WS 3rd, Li XJ, Margolis RL, Stine OC, Wagster MV, Abbott MH, Franz ML, Ranen NG. Huntington's disease gene (IT15) is widely expressed in human and rat tissues. Neuron. 1993;11(5):985–93.

[8] Nithianantharajah J, Hannan AJ. Dysregulation of synaptic proteins, dendritic spine abnormalities and pathological plasticity of synapses as experience-dependent mediators of cognitive and psychiatric symptoms in Huntington's disease. Neuroscience. 2012;

[9] Van der Burg JMM, Björkqvist M, Brundin P. Beyond the brain: widespread pathology in Huntington's disease. Lancet Neurol. 2009;8(8):765–74.

[10] Kwan W, Träger U, Davalos D, Chou A, Bouchard J, Andre R, Miller A, Weiss A, Giorgini F, Cheah C, Möller T, Stella N, Akassoglou K, Tabrizi SJ, Muchowski PJ. Mutant huntingtin impairs immune cell migration in Huntington disease. J. Clin. Invest. 2012;

[11] Björkqvist M, Wild EJ, Thiele J, Silvestroni A, Andre R, Lahiri N, Raibon E, Lee RV, Benn CL, Soulet D, Magnusson A, Woodman B, Landles C, Pouladi MA, Hayden MR, Khalili-Shirazi A, Lowdell MW, Brundin P, Bates GP, Leavitt BR, Möller T, Tabrizi SJ. A novel pathogenic pathway of immune activation detectable before clinical onset in Huntington's disease. J. Exp. Med. 2008;205(8):1869–77.

[12] Dalrymple A, Wild EJ, Joubert R, Sathasivam K, Björkqvist M, Petersén A, Jackson GS, Isaacs JD, Kristiansen M, Bates GP, Leavitt BR, Keir G, Ward M, Tabrizi SJ. Proteomic profiling of plasma in Huntington's disease reveals neuroinflammatory activation and biomarker candidates. J Proteome Res. 2007;6(7):2833–40.

[13] Leblhuber F, Walli J, Jellinger K, Tilz GP, Widner B, Laccone F, Fuchs D. Activated immune system in patients with Huntington's disease. Clin Chem Lab Med. 1998;36(10):747–50.

[14] Bouchard J, et al. Journal of Neuroscience. *in press*.

[15] Frank-Cannon TC, Alto LT, McAlpine FE, Tansey MG. Does neuroinflammation fan the flame in neurodegenerative diseases? Mol Neurodegener. 2009;4:47.

[16] Silvestroni A, Faull RLM, Strand AD, Möller T. Distinct neuroinflammatory profile in post-mortem human Huntington's disease. Neuroreport. 2009;20(12):1098–103.

[17] Simmons DA, Casale M, Alcon B, Pham N, Narayan N, Lynch G. Ferritin accumulation in dystrophic microglia is an early event in the development of Huntington's disease. Glia. 2007;55(10):1074–84.

[18] Ma L, Morton AJ, Nicholson LFB. Microglia density decreases with age in a mouse model of Huntington's disease. 2003;274–80.

[19] Tai YF, Pavese N, Gerhard A, Tabrizi SJ, Barker RA, Brooks DJ, Piccini P. Microglial activation in presymptomatic Huntington's disease gene carriers. Brain. 2007;130(Pt 7):1759–66.

[20] Politis M, Pavese N, Tai YF, Kiferle L, Mason SL, Brooks DJ, Tabrizi SJ, Barker RA, Piccini P. Microglial activation in regions related to cognitive function predicts disease onset in Huntington's disease: a multimodal imaging study. Hum Brain Mapp. 2011;32(2):258–70.

[21] Pavese N, Gerhard A, Tai YF, Ho AK, Turkheimer F, Barker RA, Brooks DJ, Piccini P. Microglial activation correlates with severity in Huntington disease: a clinical and PET study. Neurology. 2006;66(11):1638–43.

[22] Bessis A, Béchade C, Bernard D, Roumier A. Microglial control of neuronal death and synaptic properties. Glia. 2007;55(3):233–8.

[23] Graeber MB. Changing face of microglia. Science. 2010;330(6005):783–8.

[24] Wake H, Moorhouse AJ, Jinno S, Kohsaka S, Nabekura J. Resting microglia directly monitor the functional state of synapses in vivo and determine the fate of ischemic terminals. J. Neurosci. 2009;29(13):3974–80.

[25] Singhrao SK, Neal JW, Morgan BP, Gasque P. Increased complement biosynthesis by microglia and complement activation on neurons in Huntington's disease. Exp Neurol. 1999;362–76.

[26] Bonifati DM, Kishore U. Role of complement in neurodegeneration and neuroinflammation. Mol Immunol. 2007;44(5):999–1010.

[27] Stevens B, Allen NJ, Vazquez LE, Howell GR, Christopherson KS, Nouri N, Micheva KD, Mehalow AK, Huberman AD, Stafford B, Sher A, Litke AM, Lambris JD, Smith SJ, John SWM, Barres BA. The classical complement cascade mediates CNS synapse elimination. Cell. 2007;131(6):1164–78.

[28] Schwarcz R, Whetsell WO, Mangano RM. Quinolinic acid: an endogenous metabolite that produces axon-sparing lesions in rat brain. 1983;316–8.

[29] Beal MF, Ferrante RJ, Swartz KJ, Kowall NW. Chronic quinolinic acid lesions in rats closely resemble Huntington's disease. 1991;1649–59.

[30] Beal MF, Kowall NW, Ellison DW, Mazurek MF, Swartz KJ, Martin JB. Replication of the neurochemical characteristics of Huntington's disease by quinolinic acid. 1986;168–71.

[31] Guidetti P, Luthi-Carter RE, Augood SJ, Schwarcz R. Neostriatal and cortical quinolinate levels are increased in early grade Huntington's disease. Neurobiol. Dis. 2004;17(3):455–61.

[32] Guidetti P, Bates GP, Graham RK, Hayden MR, Leavitt BR, MacDonald ME, Slow EJ, Wheeler VC, Woodman B, Schwarcz R. Elevated brain 3-hydroxykynurenine and quinolinate levels in Huntington disease mice. Neurobiology of Disease. 2006;23(1):190–7.

[33] Beal MF, Matson WR, Swartz KJ, Gamache PH, Bird ED. Kynurenine pathway measurements in Huntington's disease striatum: evidence for reduced formation of kynurenic acid. 1990;1327–39.

[34] Campesan S, Green EW, Breda C, Sathyasaikumar KV, Muchowski PJ, Schwarcz R, Kyriacou CP, Giorgini F. The kynurenine pathway modulates neurodegeneration in a Drosophila model of Huntington's disease. Curr. Biol. 2011;21(11):961–6.

[35] Green EW, Campesan S, Breda C, Sathyasaikumar KV, Muchowski PJ, Schwarcz R, Kyriacou CP, Giorgini F. Drosophila eye color mutants as therapeutic tools for Huntington disease. Fly (Austin). 2012;6(2):117–20.

[36] Zwilling D, Huang S-Y, Sathyasaikumar KV, Notarangelo FM, Guidetti P, Wu H-Q, Lee J, Truong J, Andrews-Zwilling Y, Hsieh EW, Louie JY, Wu T, Scearce-Levie K, Patrick C, Adame A, Giorgini F, Moussaoui S, Laue G, Rassoulpour A, Flik G, Huang Y, Muchowski JM, Masliah E, Schwarcz R, Muchowski PJ. Kynurenine 3-monooxygenase inhibition in blood ameliorates neurodegeneration. Cell. 2011;145(6):863–74.

[37] Zádori D, Nyiri G, Szonyi A, Szatmári I, Fülöp F, Toldi J, Freund TF, Vécsei L, Klivényi P. Neuroprotective effects of a novel kynurenic acid analogue in a transgenic mouse model of Huntington's disease. J Neural Transm. 2011;118(6):865–75.

[38] Wang Y, Liu H, McKenzie G, Witting PK, Stasch J-P, Hahn M, Changsirivathanathamrong D, Wu BJ, Ball HJ, Thomas SR, Kapoor V, Celermajer DS, Mellor AL, Keaney JF, Hunt NH, Stocker R. Kynurenine is an endothelium-derived relaxing factor produced during inflammation. Nat. Med. 2010;16(3):279–85.

[39] Gandhi R, Kumar D, Burns EJ, Nadeau M, Dake B, Laroni A, Kozoriz D, Weiner HL, Quintana FJ. Activation of the aryl hydrocarbon receptor induces human type 1 regulatory T cell-like and Foxp3(+) regulatory T cells. Nat. Immunol. 2010;11(9):846–53.

[40] Mezrich JD, Fechner JH, Zhang X, Johnson BP, Burlingham WJ, Bradfield CA. An Interaction between Kynurenine and the Aryl Hydrocarbon Receptor

Can Generate Regulatory T Cells. J Immunol [Internet]. 2010 [cited 2010 Aug 26]; Available from: http://www.ncbi.nlm.nih.gov/pubmed/20720200

[41] Quintana FJ, Basso AS, Iglesias AH, Korn T, Farez MF, Bettelli E, Caccamo M, Oukka M, Weiner HL. Control of T(reg) and T(H)17 cell differentiation by the aryl hydrocarbon receptor. Nature. 2008;453(7191):65–71.

[42] Löb S, Königsrainer A, Rammensee H-G, Opelz G, Terness P. Inhibitors of indoleamine-2,3-dioxygenase for cancer therapy: can we see the wood for the trees? Nat. Rev. Cancer. 2009;9(6):445–52.

[43] Opitz CA, Litzenburger UM, Sahm F, Ott M, Tritschler I, Trump S, Schumacher T, Jestaedt L, Schrenk D, Weller M, Jugold M, Guillemin GJ, Miller CL, Lutz C, Radlwimmer B, Lehmann I, Von Deimling A, Wick W, Platten M. An endogenous tumour-promoting ligand of the human aryl hydrocarbon receptor. Nature. 2011;478(7368):197–203.

Chapter 2

Genetic Deficiency of Complement Component 3 Does Not Alter Disease Progression in a Mouse Model of Huntington's Disease

Paul B. Larkin[1,2] and Paul J. Muchowski[1,2,3,4]

[1]Gladstone Institute of Neurological Disease, [2]Neuroscience Graduate Program and the [3]Departments of Biochemistry and Biophysics and Neurology, University of California, San Francisco, CA, USA. [4]The Taube-Koret Center for Huntington's Disease Research, San Francisco, CA, USA.

Abstract

Several genes and proteins of the complement cascade are present at elevated levels in brains of patients with Huntington's disease (HD). The complement cascade is well characterized as an effector arm of the immune system, and in the brain it is important for developmental synapse elimination. We hypothesized that increased levels of complement in HD brains contributes to disease progression, perhaps by contributing to synapse elimination or inflammatory signaling. We tested this hypothesis in the R6/2 mouse model of HD by crossing mice deficient in complement component 3 (C3), a crucial complement protein found at increased levels in HD brains, to R6/2 mice and monitoring behavioral and neuropathological disease progression. We found no alterations in multiple behavioral assays, weight or survival in R6/2 mice lacking C3. We also quantified the expression of several complement cascade genes in R6/2 brains and found that the large scale upregulation of complement genes observed in HD brains is not mirrored in R6/2 brains. These data show that C3 deficiency does not alter disease progression in the R6/2 mouse model of HD.

Keywords: Complement C3, Huntington Disease, Neurodegenerative Diseases, Immunity, Innate

Introduction

Huntington's Disease (HD) is an adult-onset neurodegenerative disease characterized by impaired motor control and cognitive and emotional changes [1]. The disease is inherited in an autosomal dominant fashion and is caused by expansion of a polyglutamine tract in the ubiquitously expressed protein huntingtin. Neurodegeneration is most severe in striatum and cortex, but is ultimately observed throughout the brain.

In addition to these pathological hallmarks of HD, several studies suggest that the innate immune system is activated in HD. In blood from HD patients, several cytokines and other proteins associated with innate immune activation are elevated before—in some cases several years before—disease onset, and their presence may predict disease progression [2–4]. Inflammation in the brain also predicts and correlates with disease progression. For example, microglial activation occurs before symptoms appear and increases as disease progresses [5–7]. One aspect of the innate immune response that is elevated both in the brain and in the periphery of HD patients is the complement cascade. Several proteins of this family, including C3, C4, C7 and C9 are elevated in blood from HD patients [2,3]. Microarray experiments reveal elevated transcription of multiple complement proteins in brains from early stages HD patients (Grades 0–2) [8] and immunostaining and in situ hybridization experiments show that complement proteins are produced by microglia and deposited on neurons in late stages of disease (Grades 3–4) [9,10]. Despite this accumulating evidence of

elevated levels of complement proteins in HD, cause and effect relationships between complement and disease progression i*n vivo* have not yet been investigated.

The complement cascade has been well studied outside of the brain. It consists of soluble proteases that can bind to pathogens and signal for their destruction, thus contributing to elimination of a variety of infections. Upon binding, the initiating protease of the complement cascade, generally either C3 or complement component 1q (C1q), is activated and cleaves the next protein in the cascade, thereby activating that second protease. Sequential activation of further complement proteins leads to the formation of a “C3 convertase” that drives a common series of downstream events. These events include proinflammatory signaling, receptor-mediated phagocytosis, and destruction of cell membranes by the end product of the complement cascade: the membrane attack complex. Several complement proteins can initiate the cascade, but regardless of which one does so, activation proceeds through a C3 convertase complex that contains C3 protein. Mice lacking a functional C3 gene ($C3^{-/-}$ mice) are unable to undergo normal activation of the downstream effector functions of the complement cascade and are less adept at eliminating pathogens [11]. These mice do show some downstream complement activation because other proteases can compensate for lack of C3 [12], but this compensation is incomplete.

$C3^{-/-}$ mice show several interesting brain phenotypes that may bear on the role of C3 in HD. Notably, normal developmental synapse elimination is impaired in $C3^{-/-}$ mice and in $C1q^{-/-}$ mice [13]. Wild-type (WT) mice normally have low

levels of C3 and C1q in the brain, but they can increase expression during inflammation, likely to control infection [14], and during development [13]. Increased levels of C3 and C1q in the brain during development may contribute to synapse elimination via mechanisms similar to those by which complement in the immune system mediates phagocytosis of pathogens. Recent *in vitro* data shows that C1q and C3 can bind to neurites and trigger their phagoycytic removal by microglia [15]. Even when initiated by C1q binding, this process likely depends on fragments of C3 protein that are deposited on the neurite and recognized by microglial complement receptor 3 (CR3) [15].

In addition to complement upregulation during developmental synapse elimination, complement synthesis in the brain is also upregulated in other neurodegenerative diseases, including Alzheimer's disease (AD) [16], experimental autoimmune encephalomyelitis and multiple sclerosis [17], nerve injury models [18], AIDS-associated dementia [19] and glaucoma [13]. Studies in $C3^{-/-}$ mice show that complement can have a positive or a negative role in progression of brain diseases. For example, when $C3^{-/-}$ mice were crossed to a mouse model of AD, there was increased plaque deposition and exacerbated neurodegeneration, quantified by loss of neuronal-specific nuclear protein positive neurons in the hippocampus, implying that complement C3 is beneficial in AD [20]. On the other hand, retinal ganglion cells in $C3^{-/-}$ mice are protected from retinal ischemia-reperfusion induced cell death [21], illustrating that C3 is detrimental in this context. Further, C3 outside of the brain can also impact brain health. For example, in a mouse model of multiple sclerosis, genetic ablation of

the complement C3a receptor, which mediates some of the effects of C3, attenuates disease, likely by impairing signaling in macrophages and/or T cells outside of the brain [17]. Given these mixed results, it is difficult to predict *a priori* what role the complement cascade might be playing in the brains of HD patients.

The time course of complement upregulation could offer insight into the role of the complement cascade in HD, but again the evidence is mixed, as different complement proteins are upregulated with different time courses in HD patients. Proteomic analysis of the blood of HD patients revealed that premanifest HD patients have elevated levels of complement components C4 and C7, but levels of C9 and clusterin are not altered until advanced stages of disease [3]. Similarly, microarray studies comparing brains from early stage (Grades 0–2) HD patients to controls show that patients have increased expression of several complement mRNAs, including C3 [10,22]. However, late-grade HD brains (Grades 3–4) show upregulation of a wider variety of complement related proteins, including C3 and several other components of the complement cascade, complement regulatory factors, and complement receptors [9].

The complement cascade is one of many aspects of the innate immune system that is altered in HD [23]. Any of these interconnected elements could have beneficial or detrimental effects on brain health. We chose to focus our experiments on the complement cascade because there is strong evidence that complement in the brain can play a role in neurodegeneration and because the intriguing functional role of complement in synaptic maintenance is beginning to be elucidated. Further, complement is an attractive target because it is

upregulated in HD and because efforts to develop complement inhibitors for other inflammatory diseases are already under way [24,25]. Within the complement cascade, we chose to focus on C3 because it is central to many pathways of complement activation and signaling and because several studies have shown that $C3^{-/-}$ mice are a powerful tool for manipulating brain complement activity.

To explore the role of C3 in HD, we crossed $C3^{-/-}$ mice to the R6/2 mouse model of HD and monitored disease progression. R6/2 mice transgenically express exon 1 of the mutant human gene that causes HD. These mice exhibit progressive behavioral and neuropathological deficits that culminate in premature death. While neuronal loss is not apparent in these mice, they do lose synapses over time [26,27] and this likely contributes to behavioral phenotypes. We hypothesized that R6/2;$C3^{-/-}$ mice would benefit from the absence of this powerful destructive force and would show slower disease progression than R6/2;$C3^{+/+}$ mice. However, we found that motor deficits, weight, survival and disease associated gene expression changes in R6/2 mice were unaffected by genetic deficiency of C3.

Materials and Methods

Mice.

All animals were housed and handled in accordance with the National Institutes of Health “Guide for the Care and Use of Laboratory Animals.” All studies were approved by the Institutional Animal Care and Use Committee of the University of California, San Francisco. All animals were housed in a pathogen-free barrier facility on a 12 h light/dark cycle.

R6/2 and WT mice on a mixed CBA and C57BL/6 background (stock # 002810) and $C3^{-/-}$ mice on a C57BL/6 background (stock # 003641) were obtained from The Jackson Laboratory (Bar Harbor, ME). These mice were bred and progeny were used for behavioral studies and HD associated gene expression studies. R6/2 and WT mice used for characterization of complement related genes were generated from the sixth generation backcross of male R6/2 breeders to WT C57BL/6 females.

Genotyping.

Mouse tail DNA was analyzed by PCR to determine genotype. The R6/2 transgene was amplified using the forward primer [CGC AGG CTA GGG CTG TCA ATC ATG CT] and the reverse primer [TCA TCA GCT TTT CCA GGG TCG CCA T]. The wild-type and mutant C3 alleles were amplified separately. The forward primer [GGT TGC AGC AGT CTA TGA AGG] and the reverse primer [ATC TTG AGT GCA CCA AGC C] were used to amplify the wild-type C3 allele

while the forward primer [CTT GGG TGG AGA GGC TAT TC] and the reverse primer [AGG TGA GAT GAC AGG AGA TC] were used to amplify the Neo cassette in the mutant C3 allele.

Behavioral assays.

Open field.

Spontaneous locomotor activity was measured using an automated Photobeam Activity System (San Diego Instruments, San Diego, CA). Before testing, mice were acclimated in the testing room for 1 h. During testing, mice were placed into a clear plastic testing chamber (41 x 41 x 30 cm) for 15 min. Horizontal and vertical movements were detected by photobeam arrays traversing the testing chamber. Testing chambers were cleaned with 70% alcohol after each session.

Balance beam.

The balance beam apparatus consisted of two elevated plastic platforms, approximately 53 cm high, joined by a 38 cm long plastic beam. The starting platform was open, while the finishing platform was enclosed by an opaque plastic box. To determine performance on this assay, mice were placed on the starting platform and the experimenter measured the time required for the mouse to walk across the beam to the finishing platform.

At each time point (4, 8, and 12 weeks of age), the balance beam assay began with two training trials, where the mouse was placed on the starting

platform and guided across the beam by the experimenter. Testing trials were similar, except the mouse was left to navigate the beam unaided. Each mouse received three testing trials with a large cylindrical beam (approximately 1.59 cm diameter) on the first day of training/testing, three testing trials with a medium cylindrical beam (approximately 1.27 cm diameter) on the following day and three testing trials with a small square beam (approximately 0.6 cm on each face) on the final day of the assay. Time to cross the beam was recorded for each trial and the three trials on each beam were averaged to determine the average time to cross for a given mouse on a given beam. If the mouse fell off the beam, it was placed back on the beam at the point where it fell and the time it took to fall and be replaced was subtracted from the total time for that trial. Data with the three different sized beams gave similar results, so only results from the medium sized beam are shown.

Rotarod.

The same rotarod (Med Associates ENV-577M) was used for all rotarod studies. At each time (4, 8, and 12 weeks of age), the rotarod assay began with three training trials where the rotarod was programmed to spin at a constant rate of 16 rpm. During each training trial, mice were allowed to remain on the rotarod until they fell off or until 5 min had elapsed. Testing occurred on the 4 days after training. On each day of testing, mice received three trials during which the rotarod was programmed to accelerate from 4 to 40 rpm over a period of 5 min. Mice were allowed to remain on the rotarod until they fell off or until 5 min had

elapsed. Latency to fall was recorded automatically by a photobeam beneath the rotarod. Latency to fall was averaged across all four days of testing (twelve trials total for each mouse at a given age).

Survival.

For survival studies mice were observed daily. Survival was evaluated as the time to which the mice either died spontaneously, or lost > 15% of their maximal weight.

Quantitative real-time PCR.

RNA was harvested from frozen mouse forebrain (i.e. whole brain minus cerebellum) or striatum [microdissected as described [28]] with an RNeasy Mini kit (Qiagen, USA), according to the manufacturer's instructions. RNA was immediately reverse transcribed to cDNA with Multiscribe™ reverse transcriptase (Applied Biosystems, USA) and stored at –20 °C.

For HD associated gene expression studies and quantification of C3 mRNA, quantitative real-time PCR (qPCR) was performed using FAST SYBR Green Mastermix (Applied Biosystems, USA) as provided by the manufacturer and thermal cycling was performed using an ABI Prism 7900 HT Sequence Detector (Applied Biosystems, USA) with the following program: UNG activation (50 °C for 2 min), initial denaturation (95 °C for 10 min), and then 40 cycles of denaturation (95 °C for 15 seconds) then annealing and extension (60 °C for 1 min), followed by a disassociation stage for melting curve analysis. Analysis of fluorescence

data from genes of interest and from the control genes ATP synthase subunit 5b (Atp5b), ubiquitin C (UbC) and eukaryotic initiation factor 4a2 (Aif4a2) [29] was performed using the online analysis tool QPCR [30].

For characterization of complement related genes other than C3, qPCR was performed using SYBR Green Mastermix (Applied Biosystems, USA) as provided by the manufacturer. Thermal cycling was performed using an ABI Prism 7700 Sequence Detector (Applied Biosystems, USA) with the same program described above. Amplification efficiency was calculated for each primer pair using serially diluted standards. This efficiency was used to convert threshold cycle (number of PCR cycles required to reach an arbitrary threshold fluorescence value) into relative gene expression using the efficiency corrected delta Ct method as described [31]. For each sample, expression of the gene of interest was normalized to the control gene Atp5b.

All data are expressed as a fold change compared to WT mice, and all primers are listed in Table 1. Primers were designed using the online Roche Universal Probe Library Assay Design Center (Roche Applied Science, USA) or the online tool Primer-BLAST (NCBI) except complement component C5a receptor 1 (C5aR) [32], C3 [33] and Factor B [33] primers whose sequences were taken from published literature. Primer specificity was evaluated using Primer-BLAST (NCBI) and melting curve analysis.

C3 protein levels.

To isolate protein, fresh frozen brain was homogenized in 1X TBS buffer with 1X protease inhibitor (Roche Applied Science, USA) and spun at 10,000 x *g* for 90 min at 4 °C. A Pierce BCA protein assay kit (Thermo Scientific, USA) was used to determine protein concentration in the supernatant. Blood was collected via cardiac puncture and spun in the presence of EDTA. C3 protein levels in the supernatant and in plasma were quantified using a C3 ELISA kit (ICL Inc, Portland, OR) per the manufacturer's instructions.

Statistics.

All statistical analysis was performed using Prism (Graphpad, La Jolla, CA).

Results

We sought to determine the effect of genetic deficiency of complement protein C3 on disease progression in the R6/2 transgenic mouse model of HD. To accomplish this, we crossed R6/2 mice to $C3^{-/-}$ mice. Breeding the progeny of this cross (R6/2;$C3^{+/-}$ males crossed to WT;$C3^{+/-}$ females) gave us mice of the four different genotypes we studied: WT;$C3^{+/+}$, WT;$C3^{-/-}$, R6/2;$C3^{+/+}$, and R6/2;$C3^{-/-}$.

$C3^{-/-}$ mice do not have detectable levels of C3 protein in brain

In order to verify the efficacy of genetic deletion of C3, we used an ELISA to measure C3 protein levels in brains from mice of all four genotypes we studied (n=3/genotype). These brains were dissected and striatum was used for qPCR based detection of genes associated with disease progression, while the remaining brain material was used for C3 protein detection. As expected, we were unable to detect C3 protein in brains from $C3^{-/-}$ mice on either a WT or R6/2 background (Fig. 1A).

C3 genotype does not alter behavioral deficits in R6/2 mice

We chose to evaluate behaviors at 4, 8, and 12 weeks of age. These ages correspond to early-, mid- and late-stage disease, respectively [34]. The balance beam and rotarod assays are tests of motor coordination, while the open field test affords insight into general activity levels and anxiety related behavior. In each assay, the R6/2 transgene had a dramatic and age-dependent effect, as

expected (Fig. 1). However, R6/2;C3$^{-/-}$ mice were not significantly different from R6/2;C3$^{+/+}$ mice in any of the behavioral outcomes measured at any time (Fig. 1). In addition to these behavioral readouts, we saw no significant effects of C3 genotype on weight loss or survival in these mice (Fig. 1).

C3 genotype does not alter expression of genes associated with disease progression in R6/2 mice

We used qPCR to measure mRNA levels of genes associated with disease progression in the striatum of 12 week old mice. Transcriptional dysregulation is a widely recognized feature of HD and mouse models of HD. It is not clear whether or not these gene expression changes are causative to pathogenesis, but they are correlated with disease progression and therefore offer another surrogate marker of disease progression. We chose to evaluate two genes whose expression is increased and two genes whose expression is decreased by the R6/2 transgene.

Expression levels of D1 dopamine receptor (D1 DA R) and preproenkephalin (Penk) decline sharply over the course of disease in R6/2 mice and in human HD patients [35,36]. Both of these genes are expressed by medium spiny neurons that are lost in disease, and each gene could contribute to dysfunctional signaling in those neurons.

Heat shock protein 90 (Hsp90) is a member of the heat shock family of proteins and its activity may play a role in disease progression in R6/2 mice [37]. Microarray data suggests that it is upregulated in brains of R6/2 mice [22].

Similarly, caspase 3 expression is upregulated in brains of R6/2 mice and may be important for disease progression [38].

Brains from 12 week old R6/2 mice (late-stage disease) should have lower levels of D1 DA R and Penk but higher levels of Hsp90 and caspase 3 than brains from 12 week old WT mice. Our studies reproduced this expected effect of the R6/2 transgene, but also showed that, in R6/2 mice, C3 genotype did not modulate expression of these genes (Fig. 2). Unexpectedly, C3 genotype decreased expression of D1 DA R and Penk in WT mice.

In addition to genes associated with HD, we attempted to measure prothrombin gene expression because previous studies have shown that thrombin can partially compensate for loss of C3 in $C3^{-/-}$ mice [12]. However, when using primers that reliably detected prothrombin in positive control tissue (WT liver) the brain levels of this gene were below the limit of reliable detection in mice of all four genotypes (data not shown).

Complement C3 mRNA and protein levels are not altered in R6/2 mice

We used qPCR to quantify C3 mRNA expression in striatum from 4, 8, and 12 week old R6/2 and WT mice. Low levels of C3 mRNA were found at each age, but the presence of the R6/2 transgene did not significantly alter C3 expression at any age (Fig. 3; data from 4 weeks not shown).

We used a C3 ELISA to quantify C3 protein levels in brains and plasma from 8 and 12 week old R6/2 and WT mice. In both 8 and 12 week old mice, R6/2 genotype did not significantly alter C3 protein levels (Fig. 3).

Expression of many complement related genes is not altered in the brains of R6/2 mice

To gain a broader understanding of the status of the complement cascade, we used qPCR to quantify mRNA levels of complement genes in forebrains from 12 week old R6/2 and WT mice. We chose the genes to analyze from several types of genes: complement components that initiate and/or propagate activation of the complement cascade [complement components 1q, 3, 4 (C1q, C3, C4) and Factor B], downstream complement components that form the membrane attack complex [complement components 5, 6 and 9 (C5, C6, C9)], soluble and membrane-bound inhibitors of complement activation [C1 Inhibitor (C1 Inh), complement receptor-related protein y (Crry), decay accelerating factor (DAF) and Protectin], and receptors thought to be involved in complement signaling [C1q receptor 1 (C1qR aka CD93), C5aR, calreticulin, and low density lipoprotein receptor-related protein 1 (CD91)]. We observed few significant differences in gene expression (Table 2). Of note, C4, a complement gene that is highly upregulated in human HD brain samples [9,10,39], was not significantly upregulated in R6/2 mice. Generally, the large-scale upregulation of complement-related genes that is observed in human HD brains is not paralleled in late-stage R6/2 brains.

Discussion

The complement cascade is a powerful effector arm of the immune system and exerts a profound influence on disease progression in several mouse models of neurodegenerative disease. Elements of the complement cascade are upregulated in the brains of human HD patients at early and late stages of disease progression. However, our behavioral and gene expression experiments conclusively show that genetic deletion of C3 does not alter these aspects of disease progression in the R6/2 mouse model of HD.

Our data stand in contrast to work showing that $C3^{-/-}$ mice modulate pathogenesis in other models of neurodegeneration. In one example, genetic deletion of C3 exacerbates neurodegeneration in a mouse model of AD [20]. This illustrates that ubiquitous, lifelong C3 deficiency can strongly influence brain health in a setting of chronic neurodegeneration. We hypothesized that this would also be true for chronic neurodegeneration induced by expression of a fragment of the mutant htt gene that causes HD. Further, we hypothesized that C3 deficiency would likely be protective, rather than detrimental, in this model of HD because blocking complement signaling downstream of C3 using a C5aR antagonist reduces lesion size in rats injected with 3-nitroproprionic acid (3-NP), a mitochondrial toxin used to model HD [40]. Interestingly, one of the few significant complement related changes we observed in R6/2 mice is a downregulation of the C5aR. Since antagonizing this receptor is protective in the 3-NP model of HD, perhaps this decrease in C5aR expression is a compensatory

response. If so, administration of a C5aR antagonist may enhance this effect and offer protection in R6/2 mice as well.

It is possible that C3 deficiency alters disease progression in other studies but not in ours because C3 deficiency has multiple positive and negative effects that offset each other in R6/2 mice. We hypothesized that C3 could exacerbate pathogenesis by contributing to synapse loss or detrimental pro-inflammatory signaling, but C3 in the brain may also have protective effects. For example, $C3^{-/-}$ mice have reduced neurogenesis [41], while increased neurogenesis seems to be beneficial in mouse models of HD [42]. Also, $C3^{-/-}$ mice are unable to produce C3a and several studies have shown that C3a signaling can protect cells from inflammatory injury [43–45]. Alternatively, any effects of C3 deficiency, positive or negative, may be masked in R6/2 mice because immune cells, including microglia, are abnormal in HD [4]. The consequences of atypical immune cells in HD have not yet been fully explored, but they could include altered responses to complement. If such changes are present in HD but not in other neurodegenerative conditions, then this might help explain why C3 deficiency modulates pathogenesis in other degenerative conditions but not in the R6/2 model of HD.

The lack of effect of C3 deficiency in our study implies that there are important differences between our study and related studies where manipulations of complement do impact neurodegeneration. One feature that is seen in many such studies but absent in our experiments is significant complement upregulation. In AD and mouse models of AD, many complement components in

the brain will bind to aggregated extracellular amyloid beta and indeed studies suggest that altering complement activity in AD brain alters removal of these plaques [46]. Though mutant huntingtin does aggregate, the intracellular location of these aggregates decreases their availability for binding by complement and thus removes one stimulus that could trigger complement activation. However, there is complement upregulation both in human HD and in the 3NP model of HD despite the presumed absence of extracellular protein aggregates. This complement cascade upregulation may be in response to unknown cues, perhaps similar to those that activate complement synthesis during development. A second possibility is that complement in HD brains and in the 3NP model of HD is upregulated in response to neuronal death. The complement cascade is involved in removing dead or damaged cells throughout the body, and may play that role in the brain as well. There is significant neuronal death in human HD brains and in brains of rats injected with 3-NP, but there is little neuronal death in the R6/2 mouse model of HD. A third possible explanation for the lack of complement upregulation in our study is that we housed our mice in sterile conditions. Immune cells from HD patients and models of HD respond abnormally to immune stimulation [4] and this initial abnormal response may be necessary for other immune system changes. If so, complement upregulation in HD patients may be the result of an interplay between the disease causing mutation and normal bouts of immune system activation that are presumably lacking in mice housed in pathogen-free colonies.

Regardless of the mechanisms governing complement expression, the discrepancy between large scale complement upregulation in HD patients and few alterations in the complement system in R6/2 mice highlights the need to use multiple animal models of disease in order to explore disease mechanisms. Specifically, any future studies of the complement system in HD should consider models other than the R6/2 mouse model in the hope that other models will more accurately reflect the status of the complement system in human HD patients. Our qPCR data, along with microarray data from other studies [22], illustrate that the complement upregulation seen in HD is not a phenomenon that is mirrored in the R6/2 mouse model of HD. Here, we have also shown that completely removing C3 does not alter disease associated behavioral and gene expression changes in R6/2 mice.

Acknowledgements

This work was supported by NS057715 and the Taube-Koret Center for Huntington's Disease Research. We are grateful to Dr. S. Pabinger (Innsbruck Medical University) for valuable assistance with the online analysis program QPCR and to G. Howard for editorial review. Behavioral data were obtained with the help of the Gladstone Institutes' Behavioral Core (supported by NIH grant P30NS065780).

References

[1] Gil JM, Rego AC. Mechanisms of neurodegeneration in Huntington's disease. Eur J Neurosci. 2008;27(11):2803–20.

[2] Leblhuber F, Walli J, Jellinger K, Tilz GP, Widner B, Laccone F, Fuchs D. Activated immune system in patients with Huntington's disease. Clin Chem Lab Med. 1998;36(10):747–50.

[3] Dalrymple A, Wild EJ, Joubert R, Sathasivam K, Björkqvist M, Petersén A, Jackson GS, Isaacs JD, Kristiansen M, Bates GP, Leavitt BR, Keir G, Ward M, Tabrizi SJ. Proteomic profiling of plasma in Huntington's disease reveals neuroinflammatory activation and biomarker candidates. J Proteome Res. 2007;6(7):2833–40.

[4] Björkqvist M, Wild EJ, Thiele J, Silvestroni A, Andre R, Lahiri N, Raibon E, Lee RV, Benn CL, Soulet D, Magnusson A, Woodman B, Landles C, Pouladi MA, Hayden MR, Khalili-Shirazi A, Lowdell MW, Brundin P, Bates GP, Leavitt BR, Möller T, Tabrizi SJ. A novel pathogenic pathway of immune activation detectable before clinical onset in Huntington's disease. J. Exp. Med. 2008;205(8):1869–77.

[5] Sapp E, Kegel KB, Aronin N, Hashikawa T, Uchiyama Y, Tohyama K, Bhide PG, Vonsattel JP, DiFiglia M. Early and progressive accumulation of reactive microglia in the Huntington disease brain. 2001;161–72.

[6] Tai YF, Pavese N, Gerhard A, Tabrizi SJ, Barker RA, Brooks DJ, Piccini P. Microglial activation in presymptomatic Huntington's disease gene carriers. Brain. 2007;130(Pt 7):1759–66.

[7] Politis M, Pavese N, Tai YF, Kiferle L, Mason SL, Brooks DJ, Tabrizi SJ, Barker RA, Piccini P. Microglial activation in regions related to cognitive function predicts disease onset in Huntington's disease: a multimodal imaging study. Hum Brain Mapp. 2011;32(2):258–70.

[8] Vonsattel JP, Myers RH, Stevens TJ, Ferrante RJ, Bird ED, Richardson EP Jr. Neuropathological classification of Huntington's disease. J. Neuropathol. Exp. Neurol. 1985;44(6):559–77.

[9] Singhrao SK, Neal JW, Morgan BP, Gasque P. Increased complement biosynthesis by microglia and complement activation on neurons in Huntington's disease. Exp Neurol. 1999;362–76.

[10] Hodges A, Strand AD, Aragaki AK, Kuhn A, Sengstag T, Hughes G, Elliston LA, Hartog C, Goldstein DR, Thu D, Hollingsworth ZR, Collin F, Synek B, Holmans PA, Young AB, Wexler NS, Delorenzi M, Kooperberg C, Augood

SJ, Faull RLM, Olson JM, Jones L, Luthi-Carter R. Regional and cellular gene expression changes in human Huntington's disease brain. Hum Mol Genet. 2006;15(6):965–77.

[11] Wessels MR, Butko P, Ma M, Warren HB, Lage AL, Carroll MC. Studies of group B streptococcal infection in mice deficient in complement component C3 or C4 demonstrate an essential role for complement in both innate and acquired immunity. Proc Natl Acad Sci U S A. 1995;92(25):11490–4.

[12] Huber-Lang M, Sarma JV, Zetoune FS, Rittirsch D, Neff TA, McGuire SR, Lambris JD, Warner RL, Flierl MA, Hoesel LM, Gebhard F, Younger JG, Drouin SM, Wetsel RA, Ward PA. Generation of C5a in the absence of C3: a new complement activation pathway. Nat Med. 2006;12(6):682–7.

[13] Stevens B, Allen NJ, Vazquez LE, Howell GR, Christopherson KS, Nouri N, Micheva KD, Mehalow AK, Huberman AD, Stafford B, Sher A, Litke AM, Lambris JD, Smith SJ, John SWM, Barres BA. The classical complement cascade mediates CNS synapse elimination. Cell. 2007;131(6):1164–78.

[14] Francis K, van Beek J, Canova C, Neal JW, Gasque P. Innate immunity and brain inflammation: the key role of complement. Expert Rev Mol Med. 2003;5(15):1–19.

[15] Linnartz B, Kopatz J, Tenner AJ, Neumann H. Sialic acid on the neuronal glycocalyx prevents complement C1 binding and complement receptor-3-mediated removal by microglia. J. Neurosci. 2012;32(3):946–52.

[16] Akiyama H, Barger S, Barnum S, Bradt B, Bauer J, Cole GM, Cooper NR, Eikelenboom P, Emmerling M, Fiebich BL, Finch CE, Frautschy S, Griffin WS, Hampel H, Hull M, Landreth G, Lue L, Mrak R, Mackenzie IR, McGeer PL, O'Banion MK, Pachter J, Pasinetti G, Plata-Salaman C, Rogers J, Rydel R, Shen Y, Streit W, Strohmeyer R, Tooyoma I, Van Muiswinkel FL, Veerhuis R, Walker D, Webster S, Wegrzyniak B, Wenk G, Wyss-Coray T. Inflammation and Alzheimer's disease. Neurobiol Aging. 2000;21(3):383–421.

[17] Boos L, Campbell IL, Ames R, Wetsel RA, Barnum SR. Deletion of the complement anaphylatoxin C3a receptor attenuates, whereas ectopic expression of C3a in the brain exacerbates, experimental autoimmune encephalomyelitis. J. Immunol. 2004;173(7):4708–14.

[18] Aldskogius H, Liu L, Svensson M. Glial responses to synaptic damage and plasticity. J Neurosci Res. 1999;58(1):33–41.

[19] Bruder C, Hagleitner M, Darlington G, Mohsenipour I, Würzner R, Höllmüller I, Stoiber H, Lass-Flörl C, Dierich MP, Speth C. HIV-1 induces complement factor C3 synthesis in astrocytes and neurons by modulation of promoter activity. Mol Immunol. 2004;40(13):949–61.

[20] Maier M, Peng Y, Jiang L, Seabrook TJ, Carroll MC, Lemere CA. Complement C3 Deficiency Leads to Accelerated Amyloid {beta} Plaque Deposition and Neurodegeneration and Modulation of the Microglia/Macrophage Phenotype in Amyloid Precursor Protein Transgenic Mice. J. Neurosci. 2008;28(25):6333–41.

[21] Kuehn MH, Kim CY, Jiang B, Dumitrescu AV, Kwon YH. Disruption of the complement cascade delays retinal ganglion cell death following retinal ischemia-reperfusion. Exp Eye Res. 2008;87(2):89–95.

[22] Kuhn A, Goldstein DR, Hodges A, Strand AD, Sengstag T, Kooperberg C, Becanovic K, Pouladi MA, Sathasivam K, Cha J-HJ, Hannan AJ, Hayden MR, Leavitt BR, Dunnett SB, Ferrante RJ, Albin R, Shelbourne P, Delorenzi M, Augood SJ, Faull RLM, Olson JM, Bates GP, Jones L, Luthi-Carter R. Mutant huntingtin's effects on striatal gene expression in mice recapitulate changes observed in human Huntington's disease brain and do not differ with mutant huntingtin length or wild-type huntingtin dosage. Hum Mol Genet. 2007;16(15):1845–61.

[23] Soulet D, Cicchetti F. The role of immunity in Huntington's disease. Mol. Psychiatry. 2011;16(9):889–902.

[24] Ricklin D, Lambris JD. Complement-targeted therapeutics. Nat Biotechnol. 2007;25(11):1265–75.

[25] Qu H, Ricklin D, Lambris JD. Recent developments in low molecular weight complement inhibitors. Mol. Immunol. 2009;47(2-3):185–95.

[26] Klapstein GJ, Fisher RS, Zanjani H, Cepeda C, Jokel ES, Chesselet MF, Levine MS. Electrophysiological and morphological changes in striatal spiny neurons in R6/2 Huntington's disease transgenic mice. J Neurophysiol. 2001;86(6):2667–77.

[27] Cepeda C, Hurst RS, Calvert CR, Hernández-Echeagaray E, Nguyen OK, Jocoy E, Christian LJ, Ariano MA, Levine MS. Transient and progressive electrophysiological alterations in the corticostriatal pathway in a mouse model of Huntington's disease. J Neurosci. 2003;23(3):961–9.

[28] Chiu K, Lau WM, Lau HT, So K-F, Chang RC-C. Micro-dissection of rat brain for RNA or protein extraction from specific brain region. J Vis Exp. 2007;(7):269.

[29] Benn CL, Fox H, Bates GP. Optimisation of region-specific reference gene selection and relative gene expression analysis methods for pre-clinical trials of Huntington's disease. Mol Neurodegener. 2008;3:17.

[30] Pabinger S, Thallinger GG, Snajder R, Eichhorn H, Rader R, Trajanoski Z. QPCR: Application for real-time PCR data management and analysis. BMC Bioinformatics. 2009;10:268–268.

[31] Bookout AL, Cummins CL, Mangelsdorf DJ, Pesola JM, Kramer MF. High-Throughput Real-Time Quantitative Reverse Transcription PCR. Current Protocols in Molecular Biology. 2006;15.8.1–15.8.28.

[32] Manthey HD, Thomas AC, Shiels IA, Zernecke A, Woodruff TM, Rolfe B, Taylor SM. Complement C5a inhibition reduces atherosclerosis in ApoE-/- mice. FASEB J. 2011;25(7):2447–55.

[33] Bolger MS, Ross DS, Jiang H, Frank MM, Ghio AJ, Schwartz DA, Wright JR. Complement levels and activity in the normal and LPS-injured lung. Am. J. Physiol. Lung Cell Mol. Physiol. 2007;292(3):L748–59.

[34] Menalled L, El-Khodor BF, Patry M, Suárez-Fariñas M, Orenstein SJ, Zahasky B, Leahy C, Wheeler V, Yang XW, MacDonald M, Morton AJ, Bates G, Leeds J, Park L, Howland D, Signer E, Tobin A, Brunner D. Systematic behavioral evaluation of Huntington's disease transgenic and knock-in mouse models. Neurobiol. Dis. 2009;35(3):319–36.

[35] Cha JH, Kosinski CM, Kerner JA, Alsdorf SA, Mangiarini L, Davies SW, Penney JB, Bates GP, Young AB. Altered brain neurotransmitter receptors in transgenic mice expressing a portion of an abnormal human huntington disease gene. Proc. Natl. Acad. Sci. U.S.A. 1998;95(11):6480–5.

[36] Benn CL, Butler R, Mariner L, Nixon J, Moffitt H, Mielcarek M, Woodman B, Bates GP. Genetic knock-down of HDAC7 does not ameliorate disease pathogenesis in the R6/2 mouse model of Huntington's disease. PLoS ONE. 2009;4(6):e5747.

[37] Labbadia J, Cunliffe H, Weiss A, Katsyuba E, Sathasivam K, Seredenina T, Woodman B, Moussaoui S, Frentzel S, Luthi-Carter R, Paganetti P, Bates GP. Altered chromatin architecture underlies progressive impairment of the heat shock response in mouse models of Huntington disease. J. Clin. Invest. 2011;121(8):3306–19.

[38] Chen M, Ona VO, Li M, Ferrante RJ, Fink KB, Zhu S, Bian J, Guo L, Farrell LA, Hersch SM, Hobbs W, Vonsattel JP, Cha JH, Friedlander RM. Minocycline inhibits caspase-1 and caspase-3 expression and delays mortality in a transgenic mouse model of Huntington disease. Nat. Med. 2000;6(7):797–801.

[39] Silvestroni A, Faull RLM, Strand AD, Möller T. Distinct neuroinflammatory profile in post-mortem human Huntington's disease. Neuroreport. 2009;20(12):1098–103.

[40] Woodruff TM, Crane JW, Proctor LM, Buller KM, Shek AB, de Vos K, Pollitt S, Williams HM, Shiels IA, Monk PN, Taylor SM. Therapeutic activity of C5a receptor antagonists in a rat model of neurodegeneration. FASEB J. 2006;20(9):1407–17.

[41] Rahpeymai Y, Hietala MA, Wilhelmsson U, Fotheringham A, Davies I, Nilsson A-K, Zwirner J, Wetsel RA, Gerard C, Pekny M, Pekna M. Complement: a novel factor in basal and ischemia-induced neurogenesis. EMBO J. 2006;25(6):1364–74.

[42] Winner B, Kohl Z, Gage FH. Neurodegenerative disease and adult neurogenesis. Eur. J. Neurosci. 2011;33(6):1139–51.

[43] Boos L, Szalai AJ, Barnum SR. C3a expressed in the central nervous system protects against LPS-induced shock. Neurosci. Lett. 2005;387(2):68–71.

[44] Kildsgaard J, Hollmann TJ, Matthews KW, Bian K, Murad F, Wetsel RA. Cutting edge: targeted disruption of the C3a receptor gene demonstrates a novel protective anti-inflammatory role for C3a in endotoxin-shock. J. Immunol. 2000;165(10):5406–9.

[45] Wenderfer SE, Wang H, Ke B, Wetsel RA, Braun MC. C3a receptor deficiency accelerates the onset of renal injury in the MRL/lpr mouse. Mol. Immunol. 2009;46(7):1397–404.

[46] Wyss-Coray T, Yan F, Lin AH-T, Lambris JD, Alexander JJ, Quigg RJ, Masliah E. Prominent neurodegeneration and increased plaque formation in complement-inhibited Alzheimer's mice. Proc Natl Acad Sci U S A. 2002;99(16):10837–42.

[47] Qin X, Gao B. The complement system in liver diseases. Cell. Mol. Immunol. 2006;3(5):333–40.

Figures

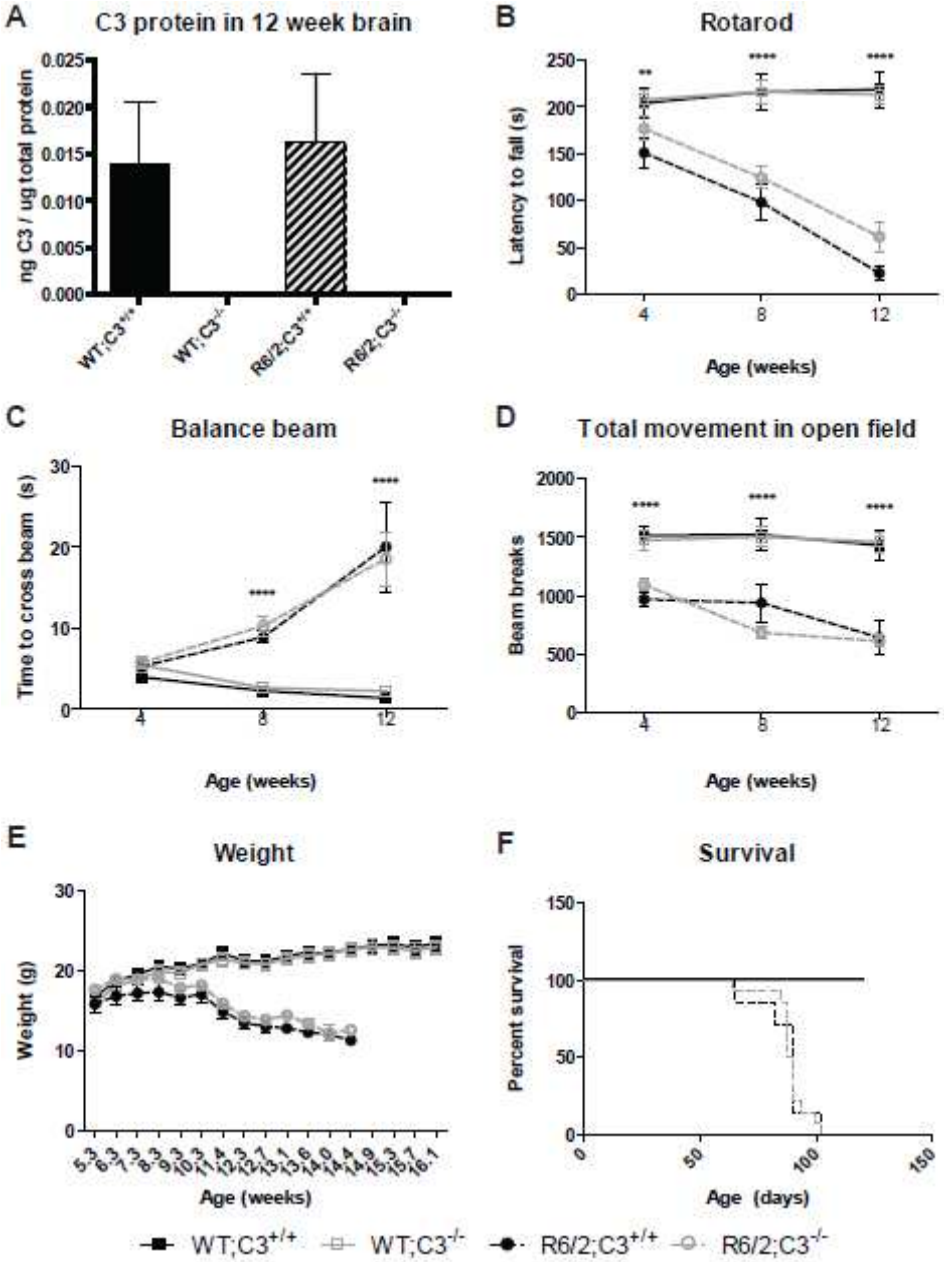

Fig. 1. Complement component 3 does not influence behavioral phenotypes in R6/2 mice. Behavioral readouts of disease progression were measured at 4, 8, and 12 weeks of age using balance beam, rotarod and open field testing. Data at each time point were tested for statistically significant differences using two-way ANOVA followed by Bonferroni post-hoc tests.

Survival was monitored throughout the study and survival curves were tested for statistically significant differences using a Log-rank (Mantel-Cox) test. At 4 weeks of age, group sizes were as follows: WT;$C3^{+/+}$ (n=15), WT;$C3^{-/-}$ (n=11), R6/2;$C3^{+/+}$ (n=7), R6/2;$C3^{-/-}$ (n=14). Error bars represent SEM. ** = p<0.01 or ****=p<0.0001 for main effect of the R6/2 transgene by two-way ANOVA.

A) C3 protein levels in brains from 12 week old mice. As expected, we were unable to detect C3 protein in brain from $C3^{-/-}$ mice. (n.d. = not detected)

B) Rotarod. R6/2 mice fall off an accelerating rotarod sooner than WT littermates (significant main effect of the R6/2 transgene at 4 weeks, $F(1,43)=7.581$, p=0.0086, 8 weeks $F(1,42)=38.91$, p<0.0001 and 12 weeks $F(1,38)=87.62$, p<0.0001 of age), but this is not affected by C3 genotype (no significant effect of C3 genotype at any age) and there is no significant interaction between the two factors.

C) Balance Beam. R6/2 mice are slower to cross an elevated balance beam than WT littermates at 8 and 12 weeks of age (significant main effect of the R6/2 transgene at 8 weeks $F(1,43)=68.36$, p<0.0001 and 12 weeks $F(1,40)=47.41$, p<0.0001 of age), but this is not affected by C3 genotype (no significant main effect of C3 genotype at any age) and there is no significant interaction between the two factors.

D) Open field. R6/2 mice are less active in an open field than WT littermates (significant main effect of the R6/2 transgene at 4 weeks $F(1,43)=38.47$, p<0.0001, 8 weeks $F(1,43)=36.83$, p<0.0001 and 12 weeks $F(1,40)=45.84$, p<0.0001 of age), but this is not affected by C3 genotype (no significant effect of

C3 genotype at any age) and there is no significant interaction between the two factors.

E) Weight. Genotype does not significantly impact weight at early time points, but R6/2 mice weigh significantly less than WT mice starting at 8.3 weeks of age (significant main effect of the R6/2 transgene $F(1,43)=6.07$, $p=0.0178$) and continuing through the course of the study. There is not a significant effect of C3 genotype at any age, and there is no significant interaction between the two factors.

F) Survival. Survival curves for R6/2;$C3^{+/+}$ and R6/2;$C3^{-/-}$ were not significantly different ($p=0.69$).

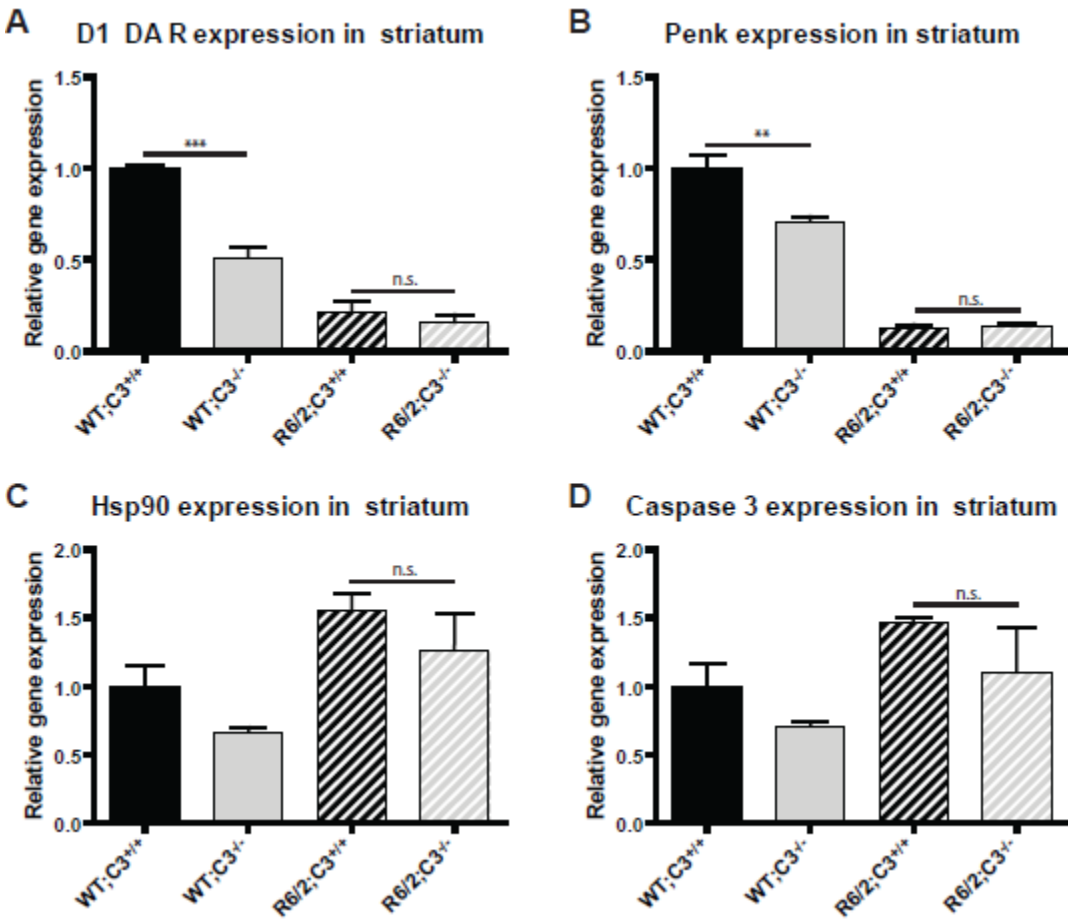

Fig. 2. C3 genotype does not alter expression of genes associated with disease progression in R6/2 mice. Littermates from each of the four genotypes tested (n=3/group) were sacrificed at 12 weeks of age (late stage of disease), and RNA was isolated from striatum. Expression of genes relevant to disease progression was measured by qPCR. Two-way ANOVA followed by Bonferroni post hoc tests shows that expression of these genes is not significantly different between R6/2;$C3^{+/+}$ and R6/2;$C3^{-/-}$ mice at this age. Error bars represent SEM. **=$p<0.01$ or ***=$p<0.001$ by Bonferroni post hoc test. n.s. = not significant.

A and B) Expression levels of D1 dopamine receptor (D1 DAR) and preproenkephalin (Penk) mRNA were lower in R6/2 mice than in WT mice, as

expected (significant main effect of the R6/2 transgene, D1 DAR $F(1,8)=151.0$, $p<0.0001$, Penk $F(1,8)=278.9$, $p<0.0001$). Unexpectedly, C3 deficiency also significantly decreased gene expression (significant main effect of C3 genotype, D1 DAR $F(1,8)=34.6$, $p=0.0004$, Penk $F(1,8)=11.12$, $p=0.01$) and there was a significant interaction between the R6/2 transgene and C3 genotype (D1 DAR $F(1,8)=21.3$, $p=0.0017$, Penk $F(1,8)=12.83$, $p=0.0072$). Using Bonferroni post hoc tests, we found that the effect of C3 genotype was confined to WT mice, as WT;$C3^{-/-}$ mice have lower levels of gene expression than WT;$C3^{+/+}$ mice (D1 DA R $p<0.001$, Penk $p<0.01$) while R6/2;$C3^{-/-}$ mice are not significantly different from R6/2;$C3^{+/+}$ mice (D1 DA R and Penk $p>0.05$).

C and D) Expression levels of Heat shock protein 90 (Hsp90) and Caspase 3 were higher in R6/2 mice than in WT mice (significant main effect of the R6/2 transgene Hsp90 $F(1,8)=11.89$, $p=0.009$, Caspase 3 $F(1,8)=5.37$, $p=0.049$) but there was no statistically significant effect of C3 genotype and no significant interaction between the R6/2 transgene and C3 genotype.

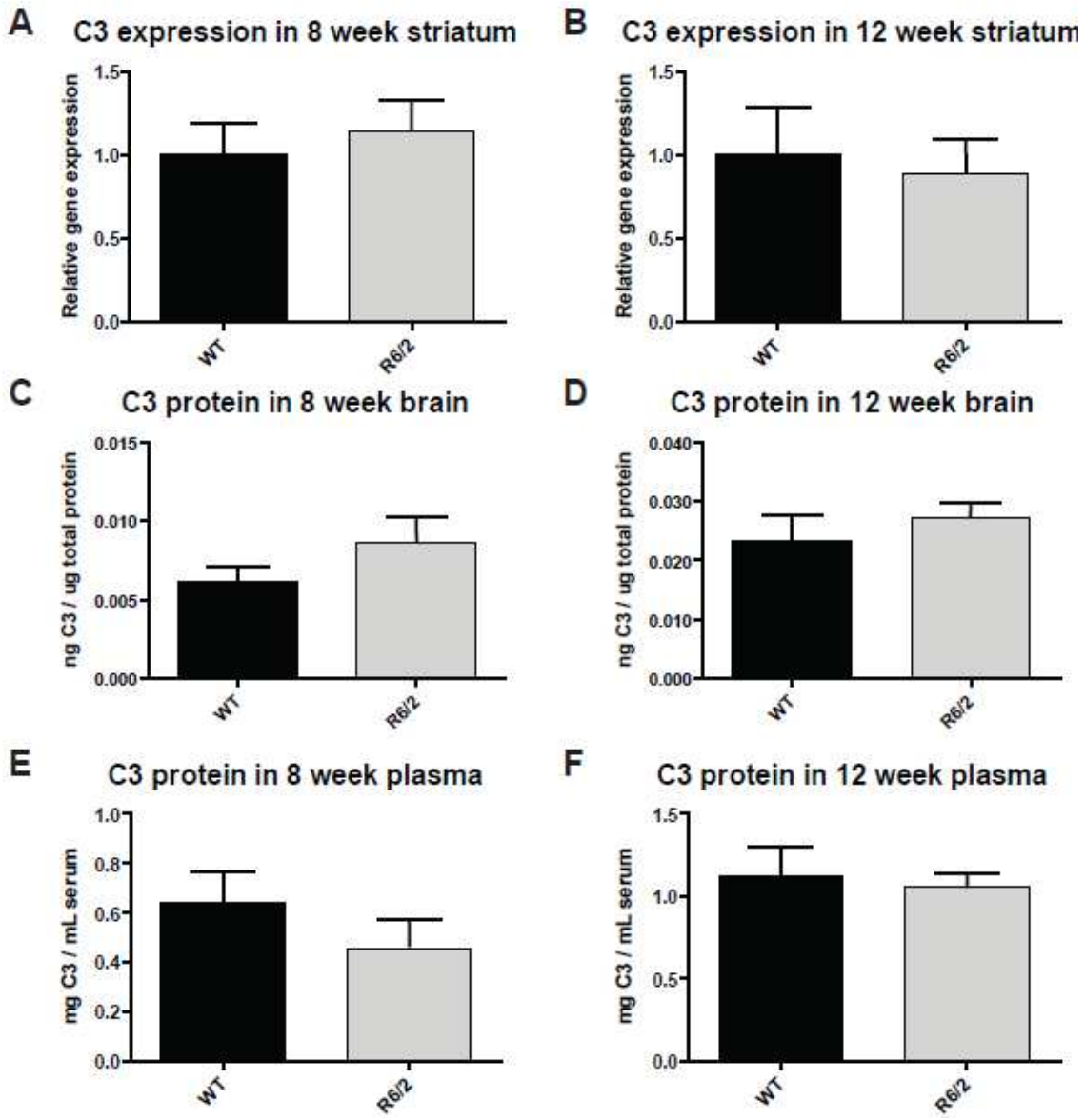

Fig. 3. Complement C3 mRNA and protein levels are not altered in R6/2 mice. R6/2 and WT littermates were sacrificed at 8 and 12 weeks of age, and mRNA and protein levels were measured. Protein levels were determined in whole brain and in plasma, while mRNA levels were measured in striatum. No significant differences were detected. Data were tested for statistically significant differences using t tests. Error bars represent SEM.

A and B) R6/2 and WT mice have similar levels of C3 mRNA expression in striatum at 8 weeks (n=4/group) and 12 weeks (n=6/group) of age.

C and D) R6/2 and WT mice have similar levels of C3 protein in brain at 8 weeks (n=5/group) and 12 weeks (n=8/group) of age.

E and F) R6/2 and WT mice have similar levels of C3 protein in plasma at 8 weeks (n=7-9/group) and 12 weeks (n=6/group) of age.

Tables

Table 1. Primers used for qPCR.

	Gene	Accession #	Forward Primer	Reverse Primer
1.	Atp5b	NM_016774	TGA GAG AGG TCC TAT CAA AAC CA	ACC AGA ATC TCC TGC TCA ACA
2.	C1 Inh	NM_009776	GAA GCT GCC TAG TGA CCA AGA	CAG CAG GAG GGT CAG TGG
3.	C1q	NM_007572	CAA GGA CTG AAG GGC GTG AA	CAA GCG TCA TTG GGT TCT GC
4.	C1qR	NM_010740	TGA AAT AGA CGC CCT GAA AAC	AAT CAA AGC CTG GGT TTA GGA
5.	C4	NM_009780	TCT CAC AAA CCC CTC GAC AT	AGC ATC CTG GAA CAC CTG AA
6.	C5	NM_010406	GGA TTC AAG CGC ATA ATA GCA	ACC CGG ATG TTG ACT CCT C
7.	C6	NM_016704	TCC AGT ACT TGA GAT GTT TAC CAG A	TTG AGG CAC GAG GTC CTT
8.	C9	NM_013485	CCG AGT AGC GGA AGA ATC AG	GGG CTC CAT CCC TAA GAT GT
9.	Calreticulin	NM_007591	TGA AGC TGT TTC CGA GTG GT	GAT GAC ATG AAC CTT CTT GGT G
10.	CD91	NM_008512	GGA CCA CCA TCG TGG AAA	TCC CAG CCA CGG TGA TAG
11.	Crry	NM_013499	GCC TTC AGT CTC TGC TCA CA	AAT TCC GTG CTG GGC TAG T
12.	DAF	NM_010016	ACT GTT GAT TGG GAC GAT GAG	TGG TGG CTC TGG ACA ATG TA
13.	Factor B	NM_001142706	GCT ACA GTC CCC AAA GTG TT	CAT GCT ATA CAC AGC CTG GA
14.	Protectin	NM_007652	GAT GCT GCC AGT TTA ACT TGT G	GAG GTC CCC AGC AAT GGT
15.	C3	NM_009778	CAC CGC CAA GAA TCG CTA C	GAT CAG GTG TTT CAG CCG C
16.	C5aR	NM_007577	GGG ATG TTG CAG CCC TTA TCA	CGC CAG ATT CAG AAA CC AG ATG
17.	Caspase 3	NM_009810	TCA TTC AGG CCT GCC GGG GT	TGG ATG AAC CAC GAC CCG TCC
18.	D1 DAR	NM_010076	TGT TTG AAA TGT TTA CAA GGT GTT C	CAG TCA GCC CTT CCT TCA GT
19.	Eif4a2	NM_013506	GAA GCC CCT CAC ATT GTT GT	GCT TCG TCC AAA ACG AAC AT
20.	Hsp90	NM_010480	AGG CTT TGC AGG CTG GTG CAG	TCC ACG ACC CAT TGG TTC ACC TGT
21.	Penk	NM_001002927	CCC AGG CGA CAT CAA TTT	TCT CCC AGA TTT TGA AAG AAG G
22.	Thrombin	NM_010168	TGG CCT GCG GCC TTT GTT CG	TCA CCT GCC AGG GGG CGA T
23.	UbC	NM_019639	AGC CCA GTG TTA CCA CCA AG	CTA AGA CAC CTC CCC CAT CA

Primers 1–14 were run with SYBR Green mastermix and an ABI 7700 thermal cycler. Primers 15–23 were run with Fast SYBR Green mastermix and an ABI 7900 HT thermal cycler. Atp5b and C3 primers were run in both sets of conditions.

Table 2. Expression of complement related genes in brain from 12 week old R6/2 and WT mice.

Gene	Function in complement cascade	Fold change in R6/2 vs. WT	p value
C1q	initiation/propagation	0.83	0.105
C3	initiation/propagation	0.94	0.861
C4	propagation of activation	1.24	0.282
Factor B	propagation of activation	0.87	0.460
C5	signaling, part of MAC	not detectable	
C6	part of MAC	not detectable	
C9	part of MAC	not detectable	
C1 Inh	soluble inhibitor	1.24	0.097
Crry	membrane bound inhibitor	0.77	0.146
DAF	membrane bound inhibitor	0.85	0.031*
Protectin	membrane bound inhibitor	0.74	0.083
C1qR	phagocytosis, receptor for C1q, MBL	0.92	0.329
C5aR	inflammatory signaling, receptor for C5a	0.72	0.005**
Calreticulin	phagocytosis, receptor for C1q, MBL	1.23	0.221
CD91	phagocytosis, receptor for C1q, MBL	1.05	0.814

Comparison of gene expression in late-stage R6/2 (n=5) and age-matched WT (n=4) forebrain. Listed p values are from t tests (*=p<0.05, **=p<0.01). For genes described as “not detectable” in these brain samples, primers were verified by their ability to detect gene expression in positive control tissue (liver) [47]. Abbreviations: MAC (Membrane Attack Complex), MBL (Mannose Binding Lectin).

Chapter 3

Indoleamine 2,3-Dioxygenase and Tryptophan 2,3-Dioxygenase Make Unique, Tissue-Specific Contributions to Basal and Inflammation Induced Kynurenine Pathway Metabolism

Paul B. Larkin[1,2*], Korrapati V. Sathyasaikumar[3*], Francesca M. Notarangelo[3], Hiroshi Funakoshi[4] Toshikazu Nakamura[4,5], Robert Schwarcz[3] & Paul J. Muchowski[1,2,6,7]

[1]Gladstone Institute of Neurological Disease, San Francisco, CA, USA.

[2]Neuroscience Graduate Program, University of California, San Francisco, CA, USA.

[3]Maryland Psychiatric Research Center, University of Maryland School of Medicine, Baltimore, Maryland, USA.

[4]Division of Molecular Regenerative Medicine, Department of Biochemistry and Molecular Biology, Osaka University Graduate School of Medicine, Osaka 565-0871, Japan.

[5]Kringle Pharma Joint Research Division for Regenerative Drug Discovery, Osaka University, Osaka 565-0871, Japan.

[6]Departments of Biochemistry and Biophysics and Neurology, University of California, San Francisco, CA, USA.

[7]The Taube-Koret Center for Huntington's Disease Research, San Francisco, CA, USA.

[*]These authors contributed equally to this study.

ABSTRACT

The kynurenine pathway (KP) of tryptophan metabolism produces a variety of bioactive metabolites that function in processes as diverse as neurodegeneration, cancer and schizophrenia. Due to their importance in these and other disease-relevant processes, pharmacological manipulation of KP activity is an active area of drug development. To safely and effectively target this pathway, it is vitally important to understand how specific KP enzymes control levels of specific bioactive metabolites. Thus, we conducted an extensive biochemical characterization of mice genetically deficient in either indoleamine 2,3-dioxygenase (IDO) or tryptophan 2,3-dioxygenase (TDO), two putative rate-limiting enzymes of the KP. These enzymes catalyze the same reaction, but differ in patterns of expression and mechanisms of regulation. We measured KP metabolite levels and enzyme activity in several tissues and in both basal and immune stimulated conditions. Our results illustrate several tissue and metabolite specific effects of KP manipulation, and are consistent with TDO-mediated control of basal KP metabolism and IDO-mediated control of immune-stimulated KP metabolism.

INTRODUCTION

The essential amino acid tryptophan can be used for protein synthesis or broken down into a variety of bioactive metabolites that have diverse roles in the brain and the immune system. Their production is controlled by the kynurenine pathway (KP), whose first and rate-limiting step is mediated by either indoleamine 2,3-dioxygenase (IDO) or tryptophan 2,3-dioxygenase (TDO) (Figure 1). Both enzymes catalyze the conversion of tryptophan to n-formyl kynurenine, which is then converted to the pivotal KP metabolite kynurenine. From kynurenine, one branch of the KP leads to formation of kynurenic acid (KYNA), and another leads to production of NAD+ via 3-hydroxykynurenine (3HK) and quinolinic acid (QUIN). Serotonin synthesis is also linked to the KP via their common substrate, tryptophan.

Over the last several decades, many studies have delved into the role of KP metabolites in brain pathology. Early studies identified 3HK and QUIN as neurotoxic KP metabolites and illustrated that their toxicity was largely due to 1) production of free radicals [both 3HK and QUIN] and 2) agonism at NMDA receptors [QUIN]. These two species can act synergistically to increase neurotoxicity [1], but interestingly KYNA can counteract their toxic effects [2]. KYNA is protective likely because it is an antagonist at glutamate receptors, including NMDA receptors.

Many neurological diseases include an altered balance between the neurotoxic,3HK- and QUIN-producing, branch of the KP and the neuroprotective

KYNA-producing branch of the KP. Brain levels of 3HK and QUIN are elevated in patients with a wide array of neurodegenerative diseases, including Alzheimer's disease, Huntington's disease, Parkinson's disease, HIV-associated dementia, and brain injury [3,4]. We recently showed that restoring the balance of these two branches by elevating brain KYNA levels ameliorates disease symptoms in mouse models of Alzheimer's disease and Huntington's disease [5]. However, pushing the balance between the two branches of the KP too far towards KYNA may also be detrimental. Brain levels of KYNA are elevated without changes in 3HK levels in patients with schizophrenia [6], and an acute rise in KYNA levels in rats causes behavioral phenotypes related to those seen in schizophrenic patients [7–9]. KYNA may alter neural signaling via its effects on glutamate receptors or its activity at more recently discovered target sites, including the α7 nicotinic acetylcholine receptor [10] and the aryl hydrocarbon receptor (AHR) [11].

While the role of KYNA binding to the AHR is not yet well defined, binding of kynurenine itself at the AHR is important for the function of the KP in the immune system. Early studies of the immune system illustrated that IDO-induced tryptophan depletion restricts growth of pathogens, while more recent studies have shown that IDO activity promotes maternal tolerance of the fetus [12]. The mechanism behind KP effects on tolerance relies, at least in part, on binding of kynurenine, and perhaps other KP metabolites, to the AHR [13,14]. This interaction leads to enhanced promotion of tolerance by regulatory T cells. Tumor cells upregulate the KP to produce more kynurenine, increase the proportion of

regulatory T cells and thus evade T cell–mediated attacks. Many studies on the KP and this mechanism of tumor promotion emphasized the role of IDO [15], but more recent work showed that TDO expression in tumor cells also has an important role [16]. Thus, inhibitors of both IDO and TDO are potential cancer therapeutics.

While inhibition of either enzyme in a tumor microenvironment may well be beneficial, systemic inhibition of each enzyme would likely have unique effects. These enzymes have biochemical differences (e.g., degree of substrate preference) [17], but they primarily differ in tissue distribution and regulation. Generally, TDO is expressed in tissues at high and stable levels primarily in the liver, but also in other organs, including brain [18,19], skin [20] and endometrium [21]. TDO activity is increased by tryptophan or decreased by downstream KP metabolites [22] and is also induced by glucocorticoids [23,24]. In contrast, IDO expression is highly variable. Often it is only present at low levels until it is induced by inflammatory immune stimulation. Basally, it is expressed most highly in epididymis and gut and at low levels in many tissues, including lung, spleen, kidney, vascular endothelium and brain [25,26]. IDO expression and activity are strongly induced in many tissues by interferon-γ, lipopolysaccharide (LPS), or a variety of other inflammatory immune stimuli [26].

A third enzyme catalyzes the conversion of tryptophan to kynurenine [27–30]. Indoleamine 2,3-dioxygenase 2 (IDO2) likely arose via gene duplication of IDO, yet the two genes differ in biochemical characteristics [31] and expression patterns [32]. The substrate affinity and activity of IDO2 appear to be lower than

those of IDO1, though assay conditions affect these differences [31]. Unlike IDO, IDO2 in mice is not induced during malaria infection, illustrating that the two enzymes respond differently to inflammatory immune stimulation [28]. The physiological relevance of IDO2 is unclear, but, like IDO and TDO, it may have a role in cancer [29].

Given the importance, number and diversity of bioactive molecules produced by the KP, pharmacological manipulation of the pathway is an active area of research aimed at both elucidation of basic biology and development o ftherapeutics for multiple indications. Mice genetically deficient in TDO (TDO KO mice) [18] or IDO (IDO KO mice) [33] provide an entry point into understanding the effects of these two critical KP enzymes. Evaluating the status of the KP in TDO KO and IDO KO mice, under basal and immune stimulated conditions, will allow us to assess the contribution of each enzyme to levels of specific bioactive KP metabolites in specific tissues.

We hypothesized that IDO KO mice have normal basal levels of KP metabolites but would be unable to upregulate KP metabolite levels in response to immune stimulation. In contrast, we hypothesized that TDO KO mice would respond normally to inflammatory immune stimulation, but would have altered basal levels of KP metabolites. We hypothesized that both the principal branches of the KP (the 3HK producing branch and the KYNA producing branch) would be regulated in concert and that liver, brain and blood would show similar changes.

To test these hypotheses, we measured a variety of outcomes related to the KP in IDO KO mice and their WT littermates and in TDO KO mice and their WT

littermates. We collected brain, liver and plasma and measured KP metabolite levels along with activity and gene expression of KP enzymes. All mice received an intraperitoneal (i.p.) injection 24 h before tissues were collected. Half the mice of each genotype received an i.p. LPS injection (inflammatory immune stimulation), and half received an i.p. saline injection. We used data from saline injected mice to determine the basal effects of gene deficiency, and we used data from LPS injected mice to measure the effect of this immune challenge in WT and KO mice. Our results illustrate several tissue and metabolite specific effects of these KP manipulations, and are largely consistent with the hypothesis that TDO controls basal KP metabolism while IDO controls immune stimulated KP metabolism.

EXPERIMENTAL PROCEDURES

Mice—All animals were housed and handled in accordance with the National Institutes of Health “Guide for the Care and Use of Laboratory Animals.” All studies were approved by the Institutional Animal Care and Use Committee of the University of California, San Francisco. All animals were housed in a pathogen-free barrier facility on a 12 h light/dark cycle.

IDO KO mice on a C57BL/6 background were obtained from The Jackson Laboratory (Bar Harbor, ME). TDO KO mice on a C57BL/6 background were generated in our laboratory [34]. For each strain, heterozygote-to-heterozygote breedings provided KO mice and wild-type (WT) littermates. All assays involved n=8–10 mice per group.

LPS Injection and Tissue Collection—LPS from *Escherichia coli* K-235 was purchased from Sigma (Sigma-Aldrich, USA, #L2143). LPS was from lot #020M4060, which was assayed at 500,000 EU/mg (Sigma). On the day of injection a fresh LPS solution was prepared using sterile saline. Mice receiving LPS treatment received one i.p. injection at a dose of 1 mg/kg. Control mice received an equal volume of saline. Mice were sacrificed 24 h post injection with an avertin overdose, followed by saline perfusion. Tissues, except blood, were collected onto dry ice and stored at -80 ℃ for all assays. Brain was dissected into forebrain and cerebellum, and all assays used forebrain. Blood was collected via cardiac puncture and spun in the presence of EDTA to obtain plasma.

Genotyping—Mouse tail DNA was analyzed by PCR to determine genotype. The WT and mutant IDO alleles were amplified in the same reaction with the forward [TGG AGC TGC CCG ACG C] and reverse primers [TAC CTT CCG AGC CCA GAC AC] for the WT allele and the forward [CTT GGG TGG AGA GGC TAT TC] and reverse primers [AGG TGA GAT GAC AGG AGA TC] for the mutant IDO allele. The WT and mutant TDO alleles were amplified in separate reactions. The forward [AGC AAA CCT GTG TGG TCC TG] and reverse primers [GCC ATA GAT AAG TCC TCC T] were used to amplify the WT TDO allele while the forward primer [CTT GGG TGG AGA GGC TAT TC] and the reverse primer [AGG TGA GAT GAC AGG AGA TC] were used to amplify the Neo cassette in the mutant TDO allele.

Chemicals—NADPH (tetrasodium salt) was purchased from Axxora (San Diego, CA). [$^{2}H_{6}$]-L-kynurenine, pentafluoropropionic anhydride (PFPA) and 2,2,3,3,3-pentafluoro-1-propanol (PFP) were obtained from Sigma-Aldrich. Ro 61-8048 was a generous gift from Dr. W. Fröstl (Novartis, Basel, Switzerland). 4-Chloro-3-hydroxyanthranilic acid (4-Cl-3-HANA) was kindly provided by Drs. W.P. Todd and B.K. Carpenter (Department of Chemistry, Cornell University, Ithaca, NY). [$^{2}H_{3}$]-QUIN was purchased from Synfine Research (Richmond Hill, Ontario, Canada), and [$^{2}H_{5}$]-L-tryptophan was obtained from CDN Isotopes (Pointe-Claire, Quebec, Canada). [1-^{14}C]-3-Hydroxyanthranilic acid (6 mCi/mmol) was obtained from Dupont/New England Nuclear (Boston, MA). All other fine

biochemicals and chemicals were purchased from various commercial suppliers and were of the highest available purity.

Enzyme Activities—Forebrain (i.e., brain minus cerebellum) and liver were stored at -80 ℃. On the day of the assays, tissues were thawed, immediately homogenized 1:5 (w/v) in ultrapure water and processed as detailed below.

Kynurenine 3-Monooxygenase (KMO; E.C. 1.14.13.9)—The original tissue homogenate was diluted 1:5 (forebrain) or 1:6,000 (liver) (v/v) in 100 mM Tris–HCl buffer (pH 8.1) containing 10 mM KCl and 1 mM EDTA. Eighty µL of the preparation were incubated for 40 min at 37 ℃ in a solution containing 1 mM NADPH, 3 mM glucose-6-phosphate, 1 U/ml glucose-6 phosphate dehydrogenase, 100 µM L-kynurenine, 10 mM KCl and 1 mM EDTA, in a total volume of 200 µL. The reaction was stopped by the addition of 50 µL of 6% perchloric acid. Blanks were obtained by adding the KMO inhibitor Ro 61-8048 (100 µM) to the incubation solution. After centrifugation (16,000 x g; 15 min), 20 µL of the supernatant were applied to a 3 µm HPLC column (HR-80; 80 mm x 4.6 mm; ESA, Chelmsford, MA) with a mobile phase of 1.5 % acetonitrile, 0.9 % triethylamine, 0.59 % phosphoric acid, 0.27 mM EDTA and 8.9 mM sodium heptane sulfonic acid, and a flow rate of 0.5 mL/min. In the eluate, the reaction product, 3-HK, was detected electrochemically using an HTEC 500 detector (Eicom Corp., San Diego, CA; oxidation potential: +0.5 V) [35]. The retention time of 3-HK was ~11 min.

Kynureninase (E.C. 3.7.1.3)—The original tissue homogenate was diluted 1:40 (forebrain) or 1:4,000 (liver) (v/v) in 5 mM Tris-HCl buffer (pH 8.4) containing 10 mM of 2-mercaptoethanol and 50 µM pyridoxal-5'-phosphate, and 100 µL of the preparation were then incubated for 2 h at 37 °C in a solution containing 90 mM Tris-HCl buffer (pH 8.4) and 4 µM DL-3-HK, in a total volume of 200 µL. The reaction was stopped by adding 50 µL of 6% perchloric acid. To obtain blanks, tissue homogenate was added at the end of the incubation (i.e., immediately before the denaturing acid). After removing the precipitate by centrifugation (16,000 x g, 15 min), 25 µL of the resulting supernatant were applied to a 5-µm C_{18} reverse-phase HPLC column (Adsorbosil; 150 mm x 4.6 mm; Grace, Deerfield, IL) with a mobile phase of 100 mM sodium acetate (pH 5.8) and 1% acetonitrile at a flow rate of 1.0 mL/min. In the eluate, the reaction product, 3-hydroxyanthranilic acid, was detected fluorimetrically (excitation wavelength: 322 nm; emission wavelength: 414 nm; S200 fluorescence detector, Perkin-Elmer, Waltham, MA). The retention time of 3-hydroxyanthranilic acid was ~4 min.

3-Hydroxyanthranilic Acid Dioxygenase (3-HAO; E.C. 1.13.11.6)—The original tissue homogenate was diluted 1:5 (forebrain) or 1:2000 (liver) (v/v) in 60 mM MES [2-(N-morpholino)ethanesulfonic acid] buffer (pH 6.0), and 100 µL of the tissue preparation were incubated for 1 h at 37 ℃ in a solution containing 0.01% ascorbic acid, 153 µM $(FeNH_4)_2(SO_4)_3$ and 3 µM (3.4 nCi) [1-^{14}C]-3-hydroxyanthranilic acid in a total volume of 200 µL. The incubation was

terminated by adding 50 µL of 6% perchloric acid, and the product (^{14}C-QUIN) was recovered by ion-exchange chromatography (Dowex 50, H^+-form) and quantitated by liquid scintillation spectrometry [36]. Blanks were obtained by including the 3-HAO inhibitor 4-Cl-3-HANA (100 µM) in the incubation solution.

Kynurenine Aminotransferases I (KAT I; E.C. 2.6.1.64) and II (KAT II; E.C. 2.6.1.7)—The original tissue homogenate was further diluted (1:1, v/v) in 5 mM Tris-acetate buffer (pH 8.0) with 10 mM 2-mercaptoethanol and 50 µM pyridoxal-5'-phosphate, and then dialyzed overnight at 4℃ ag ainst 4 L of the same buffer.

For the determination of KAT I activity, the reaction mixture contained 150 mM AMP buffer (pH 9.5), 100 µM L-kynurenine, 1 mM pyruvate, 80 µM pyridoxal-5'-phosphate and 80 µL of the dialyzed preparation in a total volume of 200 µL. For the measurement of KAT II, we used the same reaction mixture except that 150 mM Tris-acetate buffer (pH 7.4) was substituted for the AMP buffer. Blanks were prepared by using AOAA (1 mM) in the incubation solution. After incubation at 37 ℃ for 2 h, the reaction was terminated addin g 20 µL of 50% (w/v) trichloroacetic acid and 1 mL of 0.1 N HCl, and the precipitated proteins were removed by centrifugation (16,000 x g, 10 min). After suitable dilutions of the supernatant, 20 µL were directly applied to a 3-µm C_{18} reverse phase column (80 x 4.6 mm, ESA, Chelmsford, MA), and KYNA was isocratically eluted using a mobile phase with 250 mM zinc acetate, 50 mM sodium acetate and 3% acetonitrile (pH 6.2) at a flow rate of 1 mL/min. In the eluate, KYNA was detected fluorimetrically (excitation wavelength: 344 nm; emission wavelength: 398 nm;

S200 fluorescence detector; Perkin-Elmer). The retention time of KYNA under these conditions was ~7 min.

Kynurenic Acid—Plasma was diluted (1:10, v/v), and tissues were homogenized (forebrain: 1:5, liver: 1:50; w/v) in ultrapure water, and 25 µL of 6% perchloric acid were added to 100 µL of the samples. After thorough mixing, the precipitated proteins were removed by centrifugation (16,000 x g, 15 min), and 20 µL of the resulting supernatant were subjected to HPLC analysis, and KYNA was assessed as above (see "KAT II").

3-Hydroxykynurenine—Plasma was diluted (1:2, v/v), and forebrain was homogenized (1:5, w/v) in ultrapure water, and 25 µL of 6% perchloric acid were added to 100 µL of the samples. After thorough mixing, the precipitated proteins were removed by centrifugation (16,000 x g, 15 min), and 20 µL of the resulting supernatant were subjected to HPLC analysis, and 3-HK was assessed as above (see "KMO").

Tryptophan, Kynurenine, Quinolinic Acid and 3HK—Tryptophan, kynurenine and QUIN levels in brain and liver and 3HK levels in liver were quantified by gas chromatography/mass spectrometry (GC/MS). To this end, tissues were homogenized (1:20, w/v) in an aqueous solution containing 0.1% ascorbic acid, and 50 µL of a solution with internal standards (500 nM [$^2H_5$]-L-tryptophan, 10 µM [$^2H_6$]-L-kynurenine and 50 nM [$^2H_3$]-QUIN) were added to 50 µL of the tissue

preparation, and proteins were precipitated with 50 µL of acetone. After centrifugation (13,700 x g, 5 min), 50 µL of a methanol:chloroform mixture (20:50, v/v) were added to the supernatant, and the samples were centrifuged (13,700 x g, 10 min). The upper layer was added to a glass tube and evaporated to dryness (90 min). The samples were then reacted with 120 µL of PFP and 130 µL of PFPA at 75ºC for 30 min, dried down again, and taken up in 50 µL of ethyl acetate. One µL was then injected into the GC. GC/MS analysis was carried out with a 7890A GC coupled to a 7000 MS/MS (Agilent Technologies, Santa Clara, CA), using electron capture negative chemical ionization [37].

For kynurenine measurement in plasma, 50 µL of 6% perchloric acid were thoroughly mixed with 100 µL of plasma, and the precipitated proteins were removed by centrifugation (16,000 x g, 15 min). Twenty µL of the supernatant were applied to a 3 µm C_{18} reverse phase column (HR-80; 80 mm x 4.6 mm; ESA), and kynurenine was isocratically eluted using a mobile phase of 250 mM zinc acetate, 50 mM sodium acetate and 3% acetonitrile (pH 6.2) at a flow rate of 1 mL/min. Kynurenine was detected fluorimetrically (excitation wavelength: 365 nm; emission wavelength: 480 nm; S200 fluorescence detector, Perkin-Elmer). The retention time of kynurenine under these conditions was ~6 min.

NAD+ Measurements—NAD+ levels in frozen liver samples were determined using the EnzyChrom NAD/NADH Assay Kit (BioAssay Systems, Hayward, CA), according to the manufacturer's instructions. Briefly, the assay involves a lactate dehydrogenase cycling reaction in which the colored end product can be

detected by a plate reader and optical density is converted to concentration with a standard curve.

Quantitative Real-Time PCR—RNA was harvested from frozen mouse brain or liver with an RNeasy Mini kit (Qiagen), according to the manufacturer's instructions. RNA was immediately reverse transcribed to cDNA with Multiscribe reverse transcriptase (Applied Biosystems) and stored at –20 °C.

Quantitative real-time PCR (qPCR) was performed using FAST SYBR Green Mastermix (Applied Biosystems) as provided by the manufacturer, and the thermal cycling was performed using an ABI Prism 7900 HT Sequence Detector (Applied Biosystems) with the following program: UNG activation (50 °C for 2 min), initial denaturation (95 °C for 10 min), and then 40 cycles of denaturation (95 °C for 15 seconds) then annealing and extension (60 °C for 1 min), followed by a disassociation stage for melting curve analysis. Analysis of fluorescence data from genes of interest and from the control gene □-actin was performed using the online analysis tool QPCR [38].

All data are expressed as a fold change compared to WT mice treated with saline, and all primers are listed in Supplemental Table 1. Primers were designed using the online tool Primer-BLAST (NCBI) Primer specificity was evaluated using Primer-BLAST and melting curve analysis.

Statistics—For all analyses, measurements that were more than 4 standard deviations away from the mean were considered outliers and were excluded from

analysis. All statistical tests were conducted using Prism (Graphpad, La Jolla, CA). For each assay, we used a two-factor ANOVA to test for both main effects of genotype or treatment, and interaction between these two factors. If the ANOVA revealed a significant main effect, we used Bonferroni post tests to compare group means. We also used t tests where appropriate.

RESULTS

LPS Treatment, But Not IDO Genotype, Alters Brain Tryptophan Content—We treated WT or IDO KO mice with either LPS or saline in a 2x2 factorial design. We hypothesized that the LPS injection would stimulate KP activity in WT but not IDO KO mice. An increase in KP activity could be evident starting at the first step of the KP, where tryptophan is converted to kynurenine. However, LPS injection has a wide variety of effects and many may not depend on IDO. Specifically, LPS injection increased brain tryptophan levels in all mice, regardless of IDO genotype (main effect of LPS treatment, $p=0.0010$, ANOVA) (Fig. 2A). This effect of LPS was of similar magnitude in both genotypes (no interaction, ANOVA) and is consistent with published studies showing that LPS treatment increases blood and tissue tryptophan levels via the sympathetic nervous system [39,40].

LPS Treatment and IDO Genotype Alter Brain and Plasma Kynurenine Content—Given the increase we observed in brain tryptophan levels after LPS treatment, we hypothesized that LPS treatment would increase kynurenine levels in WT mice due to both increased substrate (tryptophan) availability and increased IDO mediated KP activity. Thus, we predicted that the LPS would induce higher levels of kynurenine levels in WT mice than in IDO KO mice.

In brain, we found that LPS treatment increased kynurenine levels in WT and IDO KO mice (main effect of treatment, $p<0.0001$, ANOVA), and IDO KO mice

had lower levels of brain kynurenine than WT mice (main effect of IDO genotype, brain p=0.0088, AVOVA) (Fig. 2B). This effect of IDO genotype was driven primarily by the fact that, after treatment with LPS,IDO KO mice had significantly lower kynurenine levels than WT ($p<0.05$, ANOVA, Bonferroni post test), as we detected no significant difference in basal brain kynurenine levels. Surprisingly though, the magnitude of the LPS-induced increase in brain kynurenine was not significantly greater in WT than IDO KO mice (no interaction, ANOVA). In contrast, the increase in plasma kynurenine levels induced by LPS in WT mice was completely absent in IDO KO mice (interaction, p=0.0016, ANOVA) (Fig. 2C). IDO KO mice did not have significantly lower basal plasma kynurenine levels than WT mice when evaluated by two-factor ANOVA with Bonferroni post tests; however, basal levels were lower in IDO KO mice when evaluated using a t test (p=0.0156, uncorrected for multiple comparisons). This trend, if confirmed, is interesting because it would suggest a possible, unpredicted, role for IDO in controlling basal plasma kynurenine levels.

We also determined the brain kynurenine/tryptophan ratio for each mouse in our study. The ratio of kynurenine to tryptophan is a commonly used measure of flux through the first step of the KP, where tryptophan is converted to kynurenine. We hypothesized that IDO genotype would not alter basal kynurenine/tryptophan ratio, and that LPS treatment would increase kynurenine/tryptophan ratio only in WT mice. We observed only a non-significant trend towards an increased kynurenine/tryptophan ratio in LPS-treated WT mice and a non-significant trend towards a decrease in IDO KO mice, but this resulted in a significant interaction

between treatment and IDO genotype (p=0.0418, ANOVA) (Fig. 2D). Thus the effect of LPS on the ratio of kynurenine to tryptophan in the brain is different between WT and IDO KO mice.

Our data on tryptophan and kynurenine levels are consistent with an LPS-induced increase in flux through the first step of the KP that is attenuated in brain or prevented in plasma from IDO KO mice. We also observed that tryptophan and kynurenine changes in liver are qualitatively similar to tryptophan and kynurenine changes in brain, though none was significant (Table 1). Thus, IDO plays an important and tissue-specific role in determining kynurenine levels 24 h after LPS-mediated stimulation of the immune system.

IDO Genotype Does Not Alter Brain 5HT Content—Tryptophan that is not metabolized by the KP can be used to produce 5HT (Figure 1). We found that 5HT levels in brain and were not significantly altered by either IDO genotype or LPS treatment (Fig. 2E). Thus, the increase in brain tryptophan that we observed after LPS treatment was not sufficient to increase brain 5HT content, implying that levels of this important neurotransmitter are tightly regulated by mechanisms beyond substrate availability.

However, as reported [41], we observed that 5HIAA levels were increased by LPS treatment, and thus the 5HIAA/5HT ratio, a measure of serotonergic activity, was elevated in LPS treated mice (main effect of treatment, p<0.0001, ANOVA) (Fig. 2F). This effect of LPS was similar in both WT and IDO KO mice (no interaction, ANOVA) and implies that LPS's effect is independent of IDO.

LPS-Induced Flux Through the KP Propagates Primarily Along the 3HK-Producing Branch of the KP, Rather Than the KYNA Branch, and This Increase Is Prevented in IDO KO Mice—The kynurenine produced from tryptophan by the first step of the KP can be metabolized along one of two principal branches of the KP (Fig. 1). Either the enzyme KMO converts kynurenine to 3HK or the KAT family of enzymes converts kynurenine to KYNA. Both branches produce neuroactive metabolites, but the metabolites produced by each branch are thought to have divergent roles.

To evaluate the status of the 3HK branch of the pathway, we measured brain KMO activity, but observed no differences due to LPS treatment or IDO genotype (Table 2). Since KMO activity can be modulated by inflammatory immune stimulation [42,43] the lack of an effect of LPS was surprising, but we noted a trend towards a treatment effect ($p=0.0688$). These discrepancies might be explained by differences in dosages or time courses.

We next measured brain, liver and plasma levels of 3HK (Fig. 3A, B and C). We hypothesized that IDO genotype would not alter basal 3HK levels and that LPS treatment would increase 3HK levels only in WT mice. Our data from all three tissues were consistent with these hypotheses. The effect of LPS was different in WT and IDO KO mice (interaction, brain, $p<0.0001$, liver, $p=0.0132$, plasma, $p=0.0008$, ANOVA). While the IDO genotype did not affect 3HK basal levels ($p>0.05$, ANOVA, Bonferroni post tests), LPS induced an increase in 3HK levels in WT mice that did not occur in IDO KO mice.

Though ANOVA and a Bonferroni post test showed no significant effects of IDO genotype on basal 3HK levels in brain, IDO KO mice do have lower basal 3HK levels than WT mice when this difference is evaluated with a t test ($p=0.0080$, uncorrected for multiple comparisons). This trend, like our data on basal plasma kynurenine levels, suggests a role for IDO in controlling basal KP activity in addition to its much more prominent role in controlling LPS-stimulated KP activity.

Kynurenine that is not metabolized by the 3HK branch of the KP can be diverted to the KYNA branch of the pathway by the KAT family of enzymes. To evaluate this branch of the KP, we measured activity of KAT I and KAT II, the KAT enzymes that are most important in the brain. However, we did not see any significant effects of LPS treatment or IDO genotype on activity of KAT I or KAT II (Table 2). Next, we measured brain, liver and plasma levels of KYNA (Fig. 3D, E and F). We hypothesized that changes in KYNA levels would mirror the changes we observed in 3HK levels, as our enzyme activity experiments had given us no reason to expect that kynurenine would be preferentially diverted to either branch of the KP. Surprisingly, despite the changes we observed in kynurenine and 3HK levels, we did not observe any significant effects of IDO genotype or LPS treatment on KYNA levels. However, the effect of LPS on brain KYNA levels in WT mice were different than the effects of LPS on brain KYNA levels in IDO KO mice (interaction, $p=0.0236$, ANOVA), implying that there was a subtle IDO-mediated effect of LPS treatment on brain KYNA levels.

KP Metabolites That Are Downstream of 3HK Are Modulated by LPS and IDO Genotype in a Tissue-Specific Manner—The 3HK branch of the KP produces several metabolites, including QUIN and, ultimately, NAD+. We hypothesized that changes in levels of these metabolites would mirror changes in 3HK. This was indeed the case regarding brain QUIN. Just as with brain 3HK (Fig. 3A), we observed a significant LPS-induced increase in QUIN levels in WT brain that was absent in IDO KO brain (interaction, $p=0.0047$, ANOVA) (Fig. 4A). However, despite the LPS-induced increase in liver 3HK levels (Fig. 3B), we did not observe a significant change in liver QUIN levels (Fig. 4B). Despite this, levels of the downstream metabolite NAD+ in the liver were significantly decreased by LPS treatment (main effect of treatment, $p=0.0009$, ANOVA) (Fig. 4C). In contrast to LPS induced changes farther upstream in the KP, this LPS-induced decrease was independent of IDO genotype. This decrease is consistent with previous reports [44] and the fact that it is independent of IDO is consistent with the existence of several other cellular sources of NAD+ [45].

Activity and Expression of KP Enzymes Are Not Altered by IDO Genotype—The IDO genotype did not alter the activity (Table 2) or mRNA expression (Supplemental Table 2) of most KP enzymes in both brain and liver. LPS treatment did not alter activity of most of the enzymes either, but we noted tissue-specific effects in that LPS significantly decreased activity of 3HAO in liver, but not in brain (main effect of treatment, liver $p<0.0001$, brain $p=0.9897$). LPS altered mRNA expression of some KP-related genes and control genes

responsive to LPS, confirming the effectiveness of our LPS treatment, but there were no significant interactions between IDO genotype and LPS treatment.

Most previous studies reported increased IDO mRNA levels in the hours soon after LPS treatment, but by 24–28 h after LPS treatment, IDO mRNA levels declined to close to baseline [46–49]. In our study, brains were harvested 24 h after LPS treatment, and we observed a trend towards increased IDO mRNA levels in WT mice (Supplemental Table 2, $p=0.0540$, t test). IDO mRNA was not detectable in IDO KO mice (data not shown). We also measured TDO expression in brain and observed no differences (Supplemental Table 2). This is consistent with previous studies illustrating that TDO does not respond to inflammatory immune stimuli and it shows that IDO KO mice do not compensate for loss of IDO by upregulating TDO mRNA expression.

Basal Levels of Tryptophan and Kynurenine Are Dramatically Elevated in TDO KO Mice—Previous research suggested that TDO was responsible for most tryptophan degradation under basal conditions, but was not to modulated by inflammatory stimuli. Consistent with this role of TDO, we previously showed that TDO KO mice have elevated basal levels of tryptophan in plasma and brain [34]. Surprisingly, those experiments also revealed that TDO KO mice have elevated levels of kynurenine in the plasma.

Here we confirmed and expanded these findings. As expected, brain tryptophan levels were dramatically elevated (~ninefold) in TDO KO mice, regardless of LPS treatment (main effect of genotype, $p<0.0001$, no interaction,

ANOVA) (Fig. 5A), but plasma kynurenine levels were much less dramatically elevated (~1.5 fold) (main effect of genotype p=0.0004, no interaction, ANOVA) (Fig. 5D). Given the subtle elevation in plasma kynurenine levels, we were surprised to observe a large elevation (~sevenfold) in basal levels of brain kynurenine in TDO KO mice (main effect of genotype p<0.0001, no interaction, ANOVA) (Fig. 5B). We also measured tryptophan and kynurenine levels in liver and observed large increases in both metabolites (tryptophan: ~sixfold, kynurenine: ~4.5 fold) (Table 3).

In addition, we looked for LPS-stimulated changes. Though the magnitude and standard deviation of the LPS-induced changes in brain tryptophan and kynurenine in WT mice were similar to the WT mice from our IDO KO study, the effect of LPS on tryptophan and kynurenine was not statistically significant in brains from this cohort. This may be because the magnitude and standard deviation of this change were smaller (~1.3-fold increase) than the increase in basal tryptophan and kynurenine, and thus this smaller change is discounted by our statistical methods (two-factor ANOVA and Bonferroni post tests). However, LPS treatment increased plasma kynurenine in WT and TDO KO mice (main effect of treatment p<0.0001) (Figure 5C), and mRNA expression of genes induced by LPS (Supplemental Table 3) was elevated in LPS treated mice. Thus, we are confident that the LPS injection was functional.

While the elevation in brain tryptophan highlights the importance of TDO for basal degradation of tryptophan, the elevation in brain kynurenine implies that in the absence of tryptophan other processes lead to high levels of kynurenine in

the brain. To evaluate flux through the first step of the KP, we used our tryptophan and kynurenine data to calculate a kynurenine/tryptophan ratio for each mouse in our study. We observed a significantly lower kynurenine/tryptophan ratio in TDO KO than WT mice, regardless of LPS stimulation (main effect of genotype $p<0.0001$, no interaction, ANOVA) (Fig. 5C). This illustrated that genetic loss of TDO decreased flux through the first step of the KP.

Genetic Lack of TDO Alters Brain 5HT Content—We previously showed an increase in basal 5HT and 5HIAA levels in hippocampus and midbrain of TDO KO mice [34]. In the current study, we again observed a slight but significant increase in brain 5HT levels in TDO KO mice (significant main effect of genotype, $p=0.0233$, no interaction, ANOVA) (Fig. 5E) and a larger increase in 5HIAA (significant main effect of genotype, $p<0.0001$, no interaction, ANOVA). This led to a greater increase in 5HIAA/5HT ratio in TDO KO mice than in WT mice, with or without LPS treatment (main effect of genotype, $p<0.0001$, no interaction, ANOVA) (Fig. 5F). This illustrates that while alterations in basal 5HT may be subtle in TDO KO mice, these mice also have pronounced changes in the turnover of 5HT that might contribute to their anxiety-related phenotypes [34].

In TDO KO Mice, Enzyme Activity Is Altered Along the 3HK Branch of the KP, but Metabolite Levels Are Elevated Along Both the 3HK and KYNA Branches—The elevated levels of kynurenine in TDO KO mice can be metabolized along

either of the two principal branches of the KP (Figure 1). The KAT family of enzymes diverts kynurenine towards the KYNA branch of the KP, while KMO catalyzes the conversion of kynurenine to 3HK. We found that the activity of KAT I was unchanged and there was a slight, but significant decrease in KAT II activity in brains from TDO KO mice regardless of LPS treatment (main effect of genotype, $p=0.0150$, no interaction, ANOVA) (Table 4). Surprisingly, activity of KMO was highly upregulated in brains from TDO KO mice both basally and after LPS stimulation (main effect of genotype $p<0.0001$, no interaction, ANOVA) (Fig. 6A). This novel finding shows that brain KMO activity is dynamic and can be altered in response to other changes in the KP. Similar to our data from the IDO cohort, we observed a non-significant trend towards increased brain KMO activity after LPS treatment (main effect of treatment $p=0.1407$, no interaction, ANOVA). We also observed a significant increase in KMO activity in liver from TDO KO mice (main effect of genotype, $p=0.0037$, no interaction, ANOVA) though this increase was less pronounced than in the brain (Fig. 6B). Activity of the downstream KP enzymes KYNU and 3HAO was not altered by TDO genotype (Table 4).

We hypothesized that TDO KO mice with upregulation of KMO activity and kynurenine levels would have highly elevated levels of 3HK, the product of KMO. Further, the elevation in kynurenine could lead to increased levels of KYNA in spite of the slight decrease in KAT II activity. We found 3HK levels were indeed elevated in brain and liver of TDO KO mice (main effect of genotype, brain: $p=0.0023$, no interaction, liver: $p<0.0001$, no interaction, ANOVA) (Fig. 6C and

D). Similarly, KYNA levels were elevated in brain and liver of TDO KO mice (main effect of genotype, brain: $p<0.0001$, no interaction, liver: $p=0.0147$, no interaction, ANOVA) (Fig. 6E and F). Similar to brain and liver, plasma 3HK levels were increased in TDO KO mice (main effect of treatment, $p=0.0085$, no interaction, ANOVA) (Table 3), but plasma KYNA levels, unlike brain and liver KYNA levels, were not significantly altered in TDO KO mice (main effect of genotype $p=0.0854$, no interaction, ANOVA) (Table 3).

KP Metabolites That Are Downstream of 3HK Are Modulated by LPS and TDO Genotype in a Tissue-Specific Manner—Farther down the 3HK branch of the KP, we measured levels of QUIN and NAD+. In the brain, where we observed that both LPS and lack of TDO led to increased 3HK levels, we found that LPS treatment significantly increased QUIN levels in WT and TDO KO mice (main effect of treatment, $p=0.0001$, no interaction, ANOVA) (Fig. 7A). Surprisingly though, there was no effect of TDO genotype on brain QUIN levels (main effect of genotype, $p=0.3800$, ANOVA). Thus, elevated kynurenine and 3HK levels along with elevated KMO activity have only a limited ability to increase downstream QUIN levels in brain. In contrast, liver QUIN levels are dramatically altered in TDO KO mice. We previously observed elevations in kynurenine, 3HK and KMO activity in liver of TDO KO mice, so we predicted that liver QUIN levels would be increased in TDO KO mice as well. Surprisingly, liver QUIN levels in TDO KO mice were much lower (~4 fold), regardless of LPS treatment (significant main effect of genotype, $p<0.0001$, no interaction, ANOVA) (Fig. 7B).

We were also surprised to find that liver levels of NAD+, produced even farther down the KP, were unchanged by genetic loss of TDO (Fig. 7C). However, this is consistent with tight regulation of this key cellular cofactor by mechanisms that do not necessarily depend on the KP. Our data on levels of KP metabolites produced along the 3HK branch of the KP illustrate that one cannot necessarily predict levels of a downstream metabolite based on levels of metabolites upstream of it.

Strangely, in our cohort of IDO KO mice and their WT littermates, NAD+ levels were altered by LPS treatment but there was no effect in this cohort of TDO KO mice and their WT littermates. This may be the result of small strain differences in our two cohorts: both were nominally on a C57BL/6 background, but they came from different colonies (IDO KO mice from Medical College of Georgia, USA and TDO KO mice from Osaka University, Japan) that may have diverged over time.

Expression of KP Enzymes Is Not Altered by TDO Genotype—The TDO genotype did not alter the mRNA expression of several KP enzymes (Supplemental Table 2) in brain or liver. LPS treatment did not alter expression of most of the enzymes either, but we noted that LPS significantly increased expression of KMO and KYNU in liver (main effect of treatment, KMO, $p=0.0225$, KYNU, $p=0.0303$). LPS also altered mRNA expression of control genes responsive to LPS, confirming the effectiveness of our LPS treatment, but there were no significant interactions between TDO genotype and LPS treatment.

TDO mRNA was not detectable in TDO KO mice (data not shown). We measured IDO expression in brain and observed no differences between WT and TDO KO mice (Supplemental Table 2). This shows that TDO KO mice do not compensate for loss of TDO by upregulating IDO mRNA expression.

Comparing IDO and TDO KO Mice—When analyzing data on the status of the KP in mice lacking either IDO or TDO, we were primarily concerned with two questions. 1) Does gene knockout alter basal KP function? 2) Does gene knockout alter the ability of the KP to respond to LPS treatment? Analytically, we addressed the second question by a two-factor ANOVA to determine if the treatment and genotype interacted significantly. If yes, we could conclude that the effect of LPS treatment was different in WT mice than in KO mice and thus that the knocked out gene was important for the effect of LPS on that particular readout of KP function. To determine the effect of gene knockout on basal KP function, we used a two-factor ANOVA and Bonferroni post tests to compare WT mice treated with saline to KO mice treated with saline. If this comparison was significant, we could conclude that the knocked-out gene significantly altered basal KP function. However, in some cases, we observed that, while this post test was not significant, there was no significant interaction and a significant main effect of genotype. In these cases, the significant main effect of genotype implied that genotype significantly affected our readout without altering the response to LPS. This is a more subtle implication that the knocked out gene is likely important for basal function. Table 5 shows a summary of our data and how it

answers each of our primary questions. This table clearly shows that IDO KO mice differ from WT mice in their response to LPS, but not basally, while TDO KO mice differ from WT mice basally, but not in their response to LPS.

DISCUSSION

Our results are consistent with an important role for TDO in basal but not immune-stimulated KP activity and an important role for IDO in immune-stimulated but not basal KP activity. We observed that the primary branches of the KP are differentially affected by inflammation. Looking farther downstream, we found that even metabolites along the same branch of the pathway are not always concordantly regulated—specifically, 3HK levels—do not necessarily correlate with QUIN or NAD+ levels. KP metabolites in different tissues are also not necessarily correlated. Thus, manipulating the first step of the kynurenine pathway produces changes that propagate through the rest of the KP, but multiple tissue-specific factors modulate the effects on downstream metabolites.

One factor that complicates interpretation of our data is that WT mice did not always significantly affect LPS treatment. Generally, we believe that this is due to the “snapshot” nature of our data. Responses to LPS are dynamic, and there is no one time-point or dose that will allow us to see maximal effects of LPS for all parameters we wished to evaluate. We chose to take tissues 24 h after an LPS injection because a variety of KP metabolites are upregulated at this time. However, specific analytes (i.e., mRNA) may be declining by 24 h after LPS. Further, we chose a dose of LPS that we believed would be high enough to induce KP activity, but low enough to avoid toxicity. While a larger dose would likely have led to a larger increase in KP activity, the coordinate increase in magnitude of other LPS effects, such as changes in activity, blood pressure, or

cytokine production, may have complicated the interpretation. At the dose and time we used, there are clearly significant LPS effects on many of the parameters we assayed. Thus, we believe that individual parameters where we did not observe an LPS effect, in spite of literature to the contrary, should be evaluated in light of that literature and in light of the LPS effects we see on other parameters.

Another complicating factor is that in our TDO cohort, LPS induced changes were often dwarfed by basal changes in TDO KO mice. As our statistical methods take into account variance from all groups when assigning statistical significance to comparisons of group means, the increased variance in TDO KO mice may have washed out the more subtle changes we observed with LPS.

In our studies of IDO KO mice, the effect of LPS on brain KP metabolite levels is most pronounced along the 3HK branch of the pathway. There, we observed marked elevations in 3HK and QUIN levels in WT mice treated with LPS. These elevations were completely prevented in IDO KO mice, consistent with the straightforward interpretation that these elevations are reliant on increased IDO activity after LPS. Interestingly, we did not observe a significant elevation in KYNA levels in WT mice treated with LPS. This is surprising, as we did observe robust LPS induced increases in plasma kynurenine, and peripheral increases in kynurenine are known to induce elevations in brain KYNA levels [7–9]. Some of the divergence between the 3HK- and KYNA-producing branches of the KP might be short lived changes in enzyme activity after LPS. Specifically, others reported that mRNA of KMO, which diverts kynurenine to the 3HK branch of the

KP, is increased in microglia as early as 4 h after LPS stimulation [47], while KAT mRNA is not altered by LPS treatment [42]. However, we saw no significant increase in KMO activity at 24 h after LPS injection, so changes in enzyme activity cannot explain all of the divergence. A possible explanation is provided by the functional segregation between these two branches of the pathway [50]. In the brain in particular, the enzymes of the two branches of the KP are expressed in separate cell types. Microglia principally express KMO and enzymes of the 3HK branch, and astrocytes principally express KATs and thus produce KYNA. Intrastriatal injection of kynurenine in basal conditions leads to production of both 3HK and KYNA [50]. Thus, the inflammation induced by our LPS treatment is doing something more than simply elevating kynurenine levels in brain. One possibility is that inflammation alters transport of kynurenine across cell membranes such that the kynurenine produced after LPS injection is preferentially available to microglia, and the 3HK branch, rather than astrocytes, and the KYNA branch. Numerous transport systems govern access of kynurenine to the cell body [25], and perhaps one or several of them are differentially modified by LPS-induced inflammation. Whatever the mechanism, this divergence in the fate of kynurenine after inflammation may be relevant to neurodegenerative disease. Specifically, many neurodegenerative diseases show both evidence of neuroinflammation and a KP balance that is skewed towards the 3HK branch of the pathway rather than the KYNA branch. We showed that restoring this balance by increasing KYNA is beneficial, so understanding the mechanisms that lead to the initial imbalance could reveal

other opportunities for therapeutic manipulation of the KP. Clearly, more experiments are necessary to determine the mechanisms at work here.

In contrast to pronounced alterations in 3HK and QUIN after LPS treatment, it is interesting to note that NAD+ and 5HT levels are unchanged in IDO KO mice, compared to WT mice. This may indicate that other mechanisms compensate for the role of IDO in controlling these metabolites or that these metabolites are normally regulated independent of IDO. Though manipulating the KP can contribute to NAD+ levels in specific circumstances [51], there are multiple cellular sources of NAD+ [45], and one or more of these likely compensates for any loss associated with IDO mediated KP activity. Our data on elevated 5HT levels in TDO KO mice show that manipulations of the KP can indeed alter 5HT levels. However, our data on WT mice show that acute LPS treatment does not alter brain 5HT content. Most of our data are consistent with a role for IDO only in immune-stimulated KP activity. Thus, if LPS doesn't affect 5HT, IDO doesn't either. Regardless of the mechanisms, the fact that these two important tryptophan metabolites are not altered in IDO KO mice will make it easier to interpret any future studies in IDO KO mice. In general, our results show very little evidence of compensation for loss of IDO in brain, liver or plasma from IDO KO mice. However, previous studies showed that IDO KO mice have some compensatory mechanism to replace the tolerance-promoting effects of IDO at the maternal/fetal interface [33]. In spite of this, our results show that IDO KO mice are a good tool for specifically preventing LPS-induced increases in 3HK and QUIN. This will allow us to use IDO KO mice to understand the relevance of

this specific increase. It will also be important to learn whether or not IDO KO prevents 3HK and QUIN elevations that occur in response to other inflammatory stimuli. Again, neurodegenerative disease is of particular relevance.

Previously, we argued that a large increase in basal tryptophan levels in plasma and brain from TDO KO mice implied that TDO is the most important gene for determining the basal tryptophan levels [34]. Our current studies support this conclusion. However, exploring the consequences of TDO KO farther downstream in the KP showed that important compensatory mechanisms are active in TDO KO mice. The strongest indication of this is the large increase in basal kynurenine levels in the brains of TDO KO mice. While the increase in tryptophan indicates that tryptophan breakdown is decreased in TDO KO mice, the increase in kynurenine shows that, despite this, kynurenine is still produced. The most likely enzyme to compensate for TDO loss would be IDO, but mRNA levels of IDO in brain are unchanged in TDO KO mice, and IDO mRNA in liver is undetectable in WT and TDO KO mice (data not shown). Further, in our previous studies, there was no conversion of tryptophan to kynurenine in liver of TDO KO mice. Thus, if IDO mediates this compensatory change, it does so in tissues other than liver. However, IDO activity in another tissue might reduce tryptophan levels, though not down to WT levels, and increase kynurenine levels above WT levels. Given these opposing effects, it is not clear how IDO activity alone could explain our data, and other compensatory mechanisms are probably involved. The elevation in kynurenine levels might reflect reduced used of kynurenine. The lowered kynurenine/tryptophan ratio in TDO KO mice indicates that turnover of

kynurenine is indeed lower than in WT mice, but the magnitude of this effect is relatively small (basal kynurenine/tryptophan ratio in TDO KO mice is 82% of that in WT mice). Altered transport, degradation or storage mechanisms might contribute to tissue levels of KP metabolites in TDO KO mice. For example, compensatory kynurenine production might occur in a different cellular or subcellular location than normal kynurenine production and that could alter opportunities for downstream KP processing.

Also the activity of KP enzymes can be altered by a changed tryptophan milieu. Specifically, we showed that KMO activity is markedly upregulated in brain and liver from TDO KO mice. While increased KMO activity does not explain why levels of its substrate, kynurenine, are increased, it may help explain why levels of downstream metabolites, such as NAD+, are unaltered in TDO KO mice. Further, the increase in KMO activity is of interest because KMO activity is decreased in brains of schizophrenic patients [6,52]. Thus, studies of the mechanisms behind the increase in TDO KO mice may illuminate therapeutic approaches in schizophrenia.

In our studies of IDO and TDO mice, we found that QUIN is regulated differently in the brain and liver. In WT mice, QUIN in the brain was upregulated by LPS, while QUIN levels in the liver were not altered by LPS treatment. Further, QUIN levels were dramatically decreased in the liver of TDO KO mice, while QUIN levels in brain from TDO KO mice were equivalent to WT levels. Interestingly, 3HK, a KP metabolite that is upstream of QUIN, does not show this tissue-specific regulation, implying that the responsible mechanism acts

downstream of 3HK. The tissue-specific regulation of QUIN implies that it might have different roles in these two tissues, and understanding those roles is an area for future research. It also illustrates the more general conclusion that assessing levels of one KP metabolite in one tissue will not necessarily reveal the status of that metabolite in other tissues or the status of other metabolites in the same tissue. This complex relationship is important to consider when attempting to manipulate KP metabolite levels or when attempting to evaluate the status of the KP in a whole organism.

Our results with the TDO KO support the premise that TDO is primarily important for basal, rather than immune induced, KP metabolism. They also illustrate that there are multiple compensatory changes at work in the processing of tryptophan in these mice. Thus, these mice are likely useful primarily as a setting in which to explore mechanisms that can modulate KP metabolism. Given the number and burden of diseases that involve altered tryptophan metabolism, there are many reasons that understanding how to fine tune KP metabolism may have therapeutic implications. In contrast, our results with the IDO KO are consistent with IDO playing a role in immune stimulated but not basal tryptophan metabolism. Thus, IDO KO mice should be a good tool for investigating the function of inflammation induced increases in 3HK and QUIN.

REFERENCES

[1] Guidetti P, Schwarcz R. 3-Hydroxykynurenine potentiates quinolinate but not NMDA toxicity in the rat striatum. Eur. J. Neurosci. 1999;11(11):3857–63.

[2] Winn P, Stone TW, Latimer M, Hastings MH, Clark AJ. A comparison of excitotoxic lesions of the basal forebrain by kainate, quinolinate, ibotenate, N-methyl-D-aspartate or quisqualate, and the effects on toxicity of 2-amino-5-phosphonovaleric acid and kynurenic acid in the rat. Br. J. Pharmacol. 1991;102(4):904–8.

[3] Chen Y, Guillemin GJ. Kynurenine pathway metabolites in humans: disease and healthy States. Int J Tryptophan Res. 2009;2:1–19.

[4] Schwarcz R, Bruno JP, Muchowski PJ, Wu H-Q. Kynurenines in the mammalian brain: when physiology meets pathology. Nature Reviews. Neuroscience [Internet]. 2012 [cited 2012 Jul 19]; Available from: http://www.ncbi.nlm.nih.gov/pubmed/22678511

[5] Zwilling D, Huang S-Y, Sathyasaikumar KV, Notarangelo FM, Guidetti P, Wu H-Q, Lee J, Truong J, Andrews-Zwilling Y, Hsieh EW, Louie JY, Wu T, Scearce-Levie K, Patrick C, Adame A, Giorgini F, Moussaoui S, Laue G, Rassoulpour A, Flik G, Huang Y, Muchowski JM, Masliah E, Schwarcz R, Muchowski PJ. Kynurenine 3-monooxygenase inhibition in blood ameliorates neurodegeneration. Cell. 2011;145(6):863–74.

[6] Sathyasaikumar KV, Stachowski EK, Wonodi I, Roberts RC, Rassoulpour A, McMahon RP, Schwarcz R. Impaired kynurenine pathway metabolism in the prefrontal cortex of individuals with schizophrenia. Schizophr Bull. 2011;37(6):1147–56.

[7] Shepard PD, Joy B, Clerkin L, Schwarcz R. Micromolar brain levels of kynurenic acid are associated with a disruption of auditory sensory gating in the rat. Neuropsychopharmacology. 2003;28(8):1454–62.

[8] Erhardt S, Schwieler L, Emanuelsson C, Geyer M. Endogenous kynurenic acid disrupts prepulse inhibition. Biol. Psychiatry. 2004;56(4):255–60.

[9] Chess AC, Simoni MK, Alling TE, Bucci DJ. Elevations of endogenous kynurenic acid produce spatial working memory deficits. Schizophr Bull. 2007;33(3):797–804.

[10] Hilmas C, Pereira EF, Alkondon M, Rassoulpour A, Schwarcz R, Albuquerque EX. The brain metabolite kynurenic acid inhibits alpha7 nicotinic receptor activity and increases non-alpha7 nicotinic receptor expression: physiopathological implications. J. Neurosci. 2001;21(19):7463–73.

[11] DiNatale BC, Murray IA, Schroeder JC, Flaveny CA, Lahoti TS, Laurenzana EM, Omiecinski CJ, Perdew GH. Kynurenic acid is a potent endogenous aryl hydrocarbon receptor ligand that synergistically induces interleukin-6 in the presence of inflammatory signaling. Toxicol. Sci. 2010;115(1):89–97.

[12] Munn DH, Zhou M, Attwood JT, Bondarev I, Conway SJ, Marshall B, Brown C, Mellor AL. Prevention of allogeneic fetal rejection by tryptophan catabolism. Science. 1998;281(5380):1191–3.

[13] Gandhi R, Kumar D, Burns EJ, Nadeau M, Dake B, Laroni A, Kozoriz D, Weiner HL, Quintana FJ. Activation of the aryl hydrocarbon receptor induces human type 1 regulatory T cell-like and Foxp3(+) regulatory T cells. Nat. Immunol. 2010;11(9):846–53.

[14] Mezrich JD, Fechner JH, Zhang X, Johnson BP, Burlingham WJ, Bradfield CA. An Interaction between Kynurenine and the Aryl Hydrocarbon Receptor Can Generate Regulatory T Cells. J Immunol [Internet]. 2010 [cited 2010 Aug 26]; Available from: http://www.ncbi.nlm.nih.gov/pubmed/20720200

[15] Katz JB, Muller AJ, Prendergast GC. Indoleamine 2,3-dioxygenase in T-cell tolerance and tumoral immune escape. Immunol. Rev. 2008;222:206–21.

[16] Opitz CA, Litzenburger UM, Sahm F, Ott M, Tritschler I, Trump S, Schumacher T, Jestaedt L, Schrenk D, Weller M, Jugold M, Guillemin GJ, Miller CL, Lutz C, Radlwimmer B, Lehmann I, Von Deimling A, Wick W, Platten M. An endogenous tumour-promoting ligand of the human aryl hydrocarbon receptor. Nature. 2011;478(7368):197–203.

[17] Rafice SA, Chauhan N, Efimov I, Basran J, Raven EL. Oxidation of L-tryptophan in biology: a comparison between tryptophan 2,3-dioxygenase

and indoleamine 2,3-dioxygenase. Biochem. Soc. Trans. 2009;37(Pt 2):408–12.

[18] Kanai M, Nakamura T, Funakoshi H. Identification and characterization of novel variants of the tryptophan 2,3-dioxygenase gene: differential regulation in the mouse nervous system during development. Neurosci. Res. 2009;64(1):111–7.

[19] Miller CL, Llenos IC, Dulay JR, Barillo MM, Yolken RH, Weis S. Expression of the kynurenine pathway enzyme tryptophan 2,3-dioxygenase is increased in the frontal cortex of individuals with schizophrenia. Neurobiol. Dis. 2004;15(3):618–29.

[20] Ishiguro I, Naito J, Saito K, Nagamura Y. Skin L-tryptophan-2,3-dioxygenase and rat hair growth. FEBS Lett. 1993;329(1-2):178–82.

[21] Tatsumi K, Higuchi T, Fujiwara H, Nakayama T, Egawa H, Itoh K, Fujii S, Fujita J. Induction of tryptophan 2,3-dioxygenase in the mouse endometrium during implantation. Biochem. Biophys. Res. Commun. 2000;274(1):166–70.

[22] Schutz G, Chow E, Feigelson P. Regulatory properties of hepatic tryptophan oxygenase. J. Biol. Chem. 1972;247(17):5333–7.

[23] Danesch U, Gloss B, Schmid W, Schütz G, Schüle R, Renkawitz R. Glucocorticoid induction of the rat tryptophan oxygenase gene is mediated by two widely separated glucocorticoid-responsive elements. EMBO J. 1987;6(3):625–30.

[24] Berg T, Boman D, Seglen PO. Induction of tryptophan oxygenase in primary rat liver cell suspensions by glucocorticoid hormone. Exp. Cell Res. 1972;72(2):571–4.

[25] Ruddick JP, Evans AK, Nutt DJ, Lightman SL, Rook GAW, Lowry CA. Tryptophan metabolism in the central nervous system: medical implications. Expert Rev Mol Med. 2006;8(20):1–27.

[26] Mellor AL, Munn DH. IDO expression by dendritic cells: tolerance and tryptophan catabolism. Nat Rev Immunol. 2004;4(10):762–74.

[27] Murray MF. The human indoleamine 2,3-dioxygenase gene and related human genes. Curr. Drug Metab. 2007;8(3):197–200.

[28] Ball HJ, Sanchez-Perez A, Weiser S, Austin CJD, Astelbauer F, Miu J, McQuillan JA, Stocker R, Jermiin LS, Hunt NH. Characterization of an indoleamine 2,3-dioxygenase-like protein found in humans and mice. Gene. 2007;396(1):203–13.

[29] Metz R, Duhadaway JB, Kamasani U, Laury-Kleintop L, Muller AJ, Prendergast GC. Novel tryptophan catabolic enzyme IDO2 is the preferred biochemical target of the antitumor indoleamine 2,3-dioxygenase inhibitory compound D-1-methyl-tryptophan. Cancer Res. 2007;67(15):7082–7.

[30] Yuasa HJ, Takubo M, Takahashi A, Hasegawa T, Noma H, Suzuki T. Evolution of vertebrate indoleamine 2,3-dioxygenases. J. Mol. Evol. 2007;65(6):705–14.

[31] Austin CJD, Mailu BM, Maghzal GJ, Sanchez-Perez A, Rahlfs S, Zocher K, Yuasa HJ, Arthur JW, Becker K, Stocker R, Hunt NH, Ball HJ. Biochemical characteristics and inhibitor selectivity of mouse indoleamine 2,3-dioxygenase-2. Amino Acids. 2010;39(2):565–78.

[32] Ball HJ, Yuasa HJ, Austin CJD, Weiser S, Hunt NH. Indoleamine 2,3-dioxygenase-2; a new enzyme in the kynurenine pathway. Int. J. Biochem. Cell Biol. 2009;41(3):467–71.

[33] Baban B, Chandler P, McCool D, Marshall B, Munn DH, Mellor AL. Indoleamine 2,3-dioxygenase expression is restricted to fetal trophoblast giant cells during murine gestation and is maternal genome specific. J. Reprod. Immunol. 2004;61(2):67–77.

[34] Kanai M, Funakoshi H, Takahashi H, Hayakawa T, Mizuno S, Matsumoto K, Nakamura T. Tryptophan 2,3-dioxygenase is a key modulator of physiological neurogenesis and anxiety-related behavior in mice. Mol Brain. 2009;2(1):8.

[35] Heyes MP, Quearry BJ. Quantification of 3-hydroxykynurenine in brain by high-performance liquid chromatography and electrochemical detection. J. Chromatogr. 1988;428(2):340–4.

[36] Foster AC, White RJ, Schwarcz R. Synthesis of quinolinic acid by 3-hydroxyanthranilic acid oxygenase in rat brain tissue in vitro. J. Neurochem. 1986;47(1):23–30.

[37] Notarangelo FM, Wu H-Q, Macherone A, Graham DR, Schwarcz R. Gas chromatography/tandem mass spectrometry detection of extracellular kynurenine and related metabolites in normal and lesioned rat brain. Anal. Biochem. 2012;421(2):573–81.

[38] Pabinger S, Thallinger GG, Snajder R, Eichhorn H, Rader R, Trajanoski Z. QPCR: Application for real-time PCR data management and analysis. BMC Bioinformatics. 2009;10:268–268.

[39] Dunn AJ, Welch J. Stress-and Endotoxin-Induced Increases in Brain Tryptophan and Serotonin Metabolism Depend on Sympathetic Nervous System Activity. Journal of Neurochemistry. 1991;57(5):1615–22.

[40] Miura H, Shirokawa T, Isobe K, Ozaki N. Shifting the balance of brain tryptophan metabolism elicited by isolation housing and systemic administration of lipopolysaccharide in mice. Stress. 2009;12(3):206–14.

[41] O'Connor JC, Lawson MA, André C, Moreau M, Lestage J, Castanon N, Kelley KW, Dantzer R. Lipopolysaccharide-induced depressive-like behavior is mediated by indoleamine 2,3-dioxygenase activation in mice. Mol. Psychiatry. 2009;14(5):511–22.

[42] Connor TJ, Starr N, O'Sullivan JB, Harkin A. Induction of indolamine 2,3-dioxygenase and kynurenine 3-monooxygenase in rat brain following a systemic inflammatory challenge: a role for IFN-gamma? Neurosci. Lett. 2008;441(1):29–34.

[43] Alberati-Giani D, Ricciardi-Castagnoli P, Köhler C, Cesura AM. Regulation of the kynurenine metabolic pathway by interferon-gamma in murine cloned macrophages and microglial cells. J. Neurochem. 1996;66(3):996–1004.

[44] Moffett JR, Namboodiri MA. Tryptophan and the immune response. Immunol Cell Biol. 2003;81(4):247–65.

[45] Nikiforov A, Dölle C, Niere M, Ziegler M. Pathways and subcellular compartmentation of NAD biosynthesis in human cells: from entry of extracellular precursors to mitochondrial NAD generation. J. Biol. Chem. 2011;286(24):21767–78.

[46] O'Connor JC, Lawson MA, André C, Briley EM, Szegedi SS, Lestage J, Castanon N, Herkenham M, Dantzer R, Kelley KW. Induction of IDO by bacille Calmette-Guérin is responsible for development of murine depressive-like behavior. J. Immunol. 2009;182(5):3202–12.

[47] Corona AW, Huang Y, O'Connor JC, Dantzer R, Kelley KW, Popovich PG, Godbout JP. Fractalkine receptor (CX3CR1) deficiency sensitizes mice to the behavioral changes induced by lipopolysaccharide. J Neuroinflammation. 2010;7:93.

[48] Godbout JP, Moreau M, Lestage J, Chen J, Sparkman NL, O' Connor J, Castanon N, Kelley KW, Dantzer R, Johnson RW. Aging exacerbates depressive-like behavior in mice in response to activation of the peripheral innate immune system. Neuropsychopharmacology. 2008;33(10):2341–51.

[49] André C, O'Connor JC, Kelley KW, Lestage J, Dantzer R, Castanon N. Spatio-temporal differences in the profile of murine brain expression of proinflammatory cytokines and indoleamine 2,3-dioxygenase in response to peripheral lipopolysaccharide administration. J. Neuroimmunol. 2008;200(1-2):90–9.

[50] Amori L, Guidetti P, Pellicciari R, Kajii Y, Schwarcz R. On the relationship between the two branches of the kynurenine pathway in the rat brain in vivo. J. Neurochem. 2009;109(2):316–25.

[51] Bellac CL, Coimbra RS, Christen S, Leib SL. Inhibition of the kynurenine-NAD+ pathway leads to energy failure and exacerbates apoptosis in pneumococcal meningitis. J. Neuropathol. Exp. Neurol. 2010;69(11):1096–104.

[52] Wonodi I, Stine OC, Sathyasaikumar KV, Roberts RC, Mitchell BD, Hong LE, Kajii Y, Thaker GK, Schwarcz R. Downregulated kynurenine 3-monooxygenase gene expression and enzyme activity in schizophrenia and genetic association with schizophrenia endophenotypes. Arch. Gen. Psychiatry. 2011;68(7):665–74.

FIGURES

Figure 1.

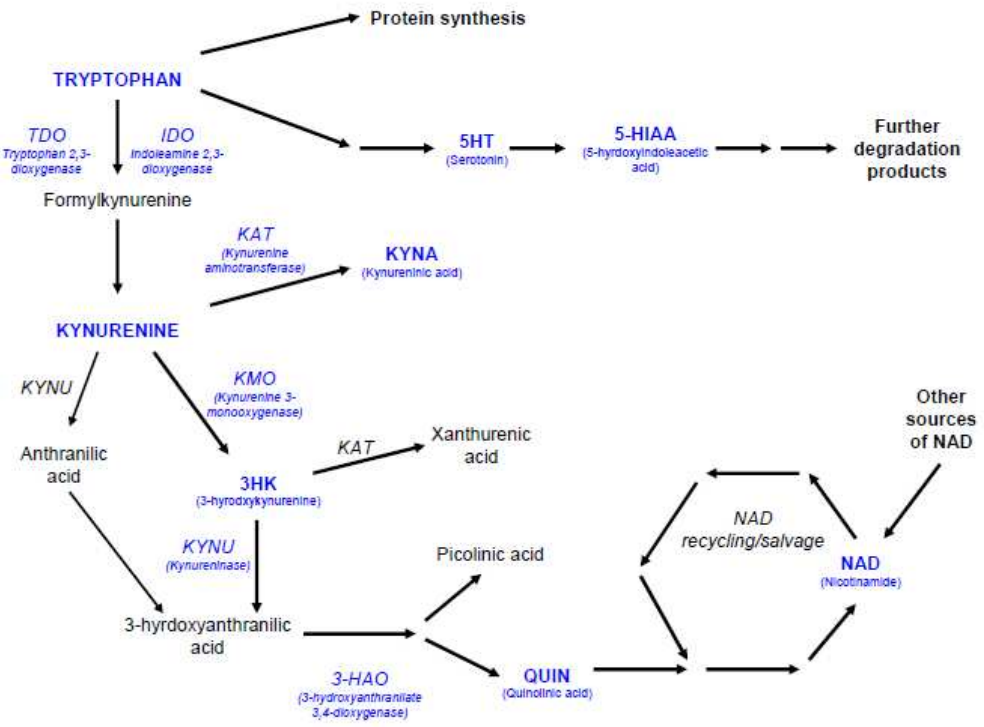

FIGURE 1. **Kynurenine pathway of tryptophan degradation in mammals.** Indoleamine 2,3-dioxygenase (IDO) and tryptophan 2,3-dioxygenase (TDO) catalyze the first step of the kynurenine pathway. This pathway contains several branches, most importantly for this study the KYNA producing branch initiated by the kynurenine aminotransferase (KAT) family enzymes and the 3HK producing branch initiated by kynurenine monooxygenase (KMO). The end product of the 3HK branch of the KP is the important cellular cofactor NAD+, and the KP is linked to serotonin synthesis by competition for a shared substrate, tryptophan. Elements measured in the current study are shown in blue.

Figure 2.

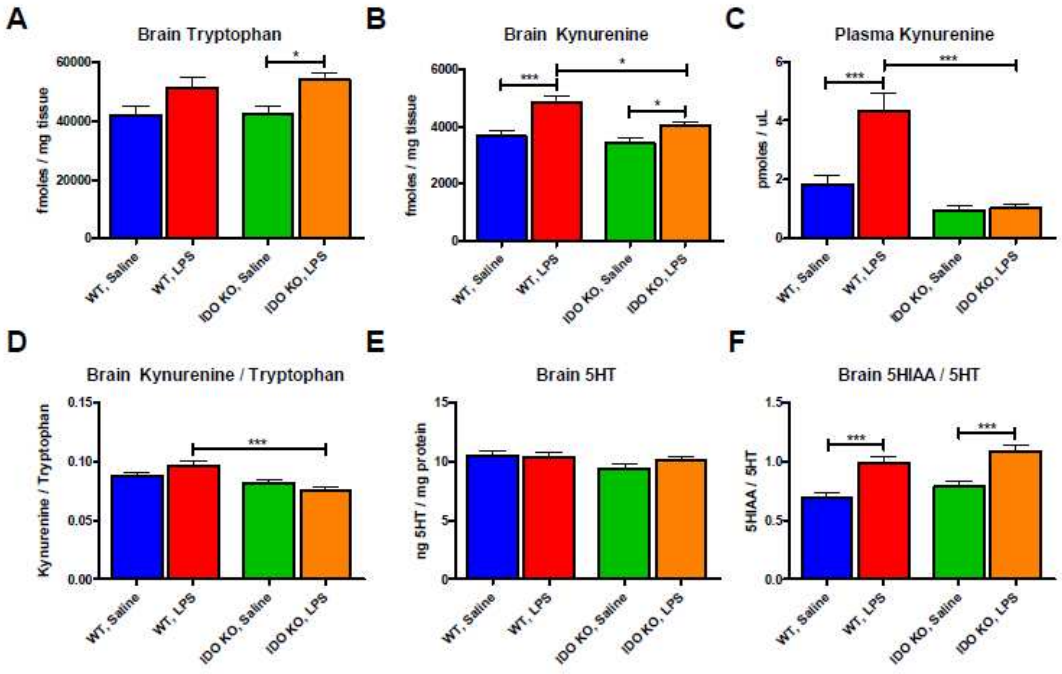

FIGURE 2. **LPS treatment alters tryptophan metabolism along both the KP and the serotonin synthesis pathway, but only the KP effects depend on IDO genotype.** *A and B*, LPS treatment increases brain tryptophan and kynurenine levels (main effect of treatment, tryptophan p=0.0010, ANOVA, kynurenine, p<0.0001, ANOVA), and this effect of LPS is not different on WT and IDO KO mice (no interaction, ANOVA). However, WT mice have significantly higher brain kynurenine levels than IDO KO mice (main effect of genotype, p=0.0088, ANOVA), and this is driven by an increase in WT mice treated with LPS compared to IDO KO mice treated with LPS (p<0.05, ANOVA, Bonferroni post test). *C*, LPS treatment increases plasma kynurenine levels in WT but not IDO KO mice (interaction, p=0.0016, ANOVA). *D*, LPS has a different effect on the ratio of brain kynurenine to brain tryptophan in WT mice than in IDO KO mice

(interaction, p=0.0418, ANOVA). *E*, LPS and IDO genotype did not affect brain levels of 5HT. *F,* LPS treatment significantly increases the ratio of 5HIAA to 5HT (main effect of treatment, p<0.0001, ANOVA), indicating increased 5HT turnover, but IDO genotype does not alter this phenomenon. * p<0.05, *** p<0.001, ANOVA, Bonferroni post test. Points represent mean, and error bars represent SEM.

Figure 3.

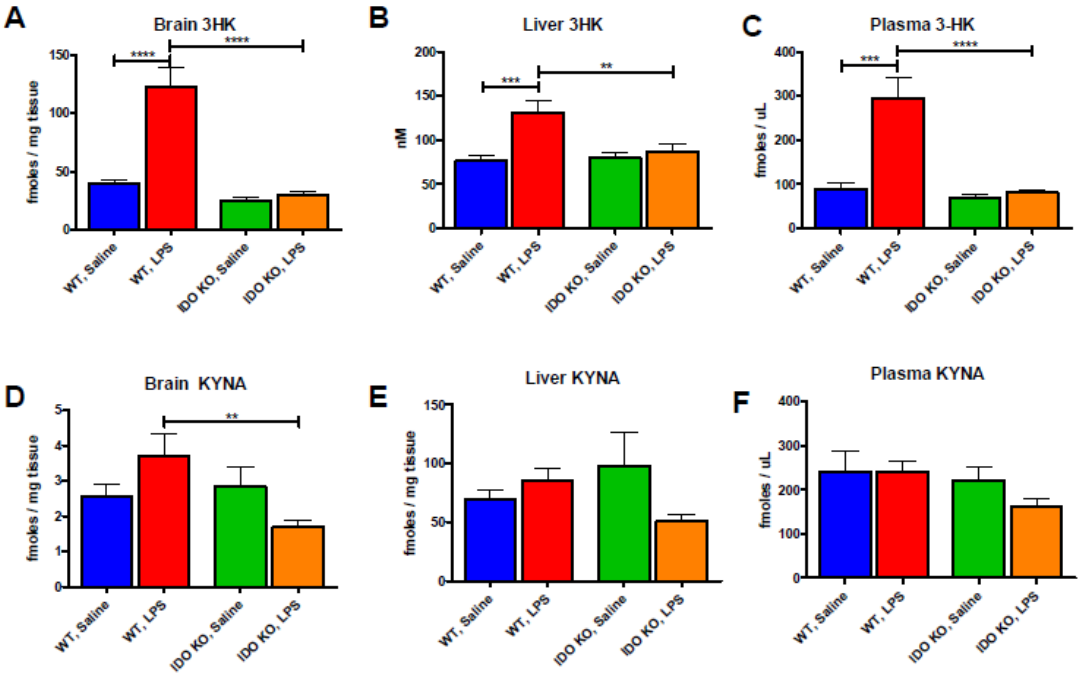

FIGURE 3. **LPS induced KP up-regulation propagates mainly along the 3HK branch of the KP, rather than the KYNA branch, and this is prevented by IDO KO.** *A–C*, LPS treatment increases 3HK levels in brain, liver and plasma from WT mice, but not in IDO KO mice (interaction, brain 3HK, $p<0.0001$, liver 3HK, $p=0.0132$, plasma 3HK, $p=0.0008$, ANOVA). *D–F*, LPS treatment does not increase KYNA levels in brain, liver or plasma from WT or IDO KO mice. However, the small, non-significant effects of LPS on brain KYNA levels are in opposite directions in WT and IDO KO mice. Thus, the significant interaction of LPS treatment and IDO genotype ($p=0.0236$, ANOVA) implies that IDO has a subtle role in controlling LPS-induced changes in brain KYNA levels. ** $p<0.01$, *** $p<0.001$, **** $p<0.0001$, ANOVA, Bonferroni post test. Points represent mean, and error bars represent SEM.

Figure 4.

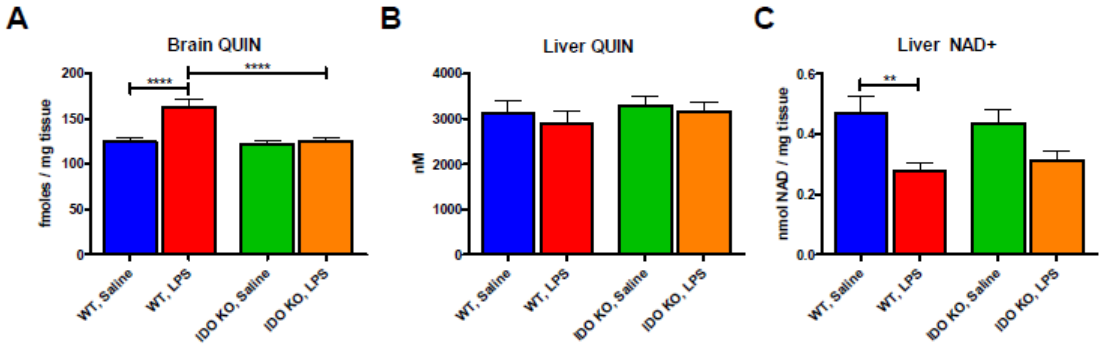

FIGURE 4. **Downstream KP metabolites are altered by LPS and IDO genotype in a tissue-specific manner.** *A*, Mirroring changes in brain 3HK levels (Figure 3A), LPS treatment increases brain QUIN levels in WT but not IDO KO mice (interaction, p=0.0047, ANOVA). *B*, In contrast to both liver 3HK levels (Figure 3 B) and brain QUIN levels (Figure 4 A), LPS treatment does not alter liver QUIN levels in either WT or IDO KO mice. *C*, There is no effect of IDO genotype on liver NAD+ levels, and the effect of LPS is not significantly different between WT and IDO KO mice (no interaction, ANOVA). ** p<0.01, **** p<0.0001, ANOVA, Bonferroni post test. Points represent mean, and error bars represent SEM.

Figure 5.

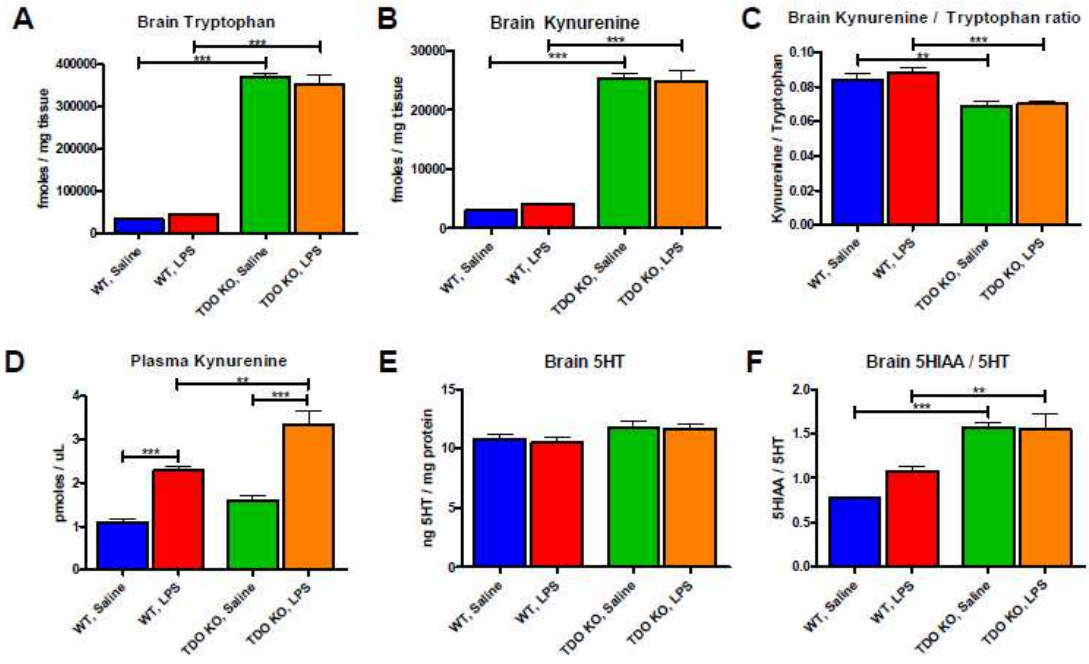

FIGURE 5. **TDO KO mice have dramatically altered basal tryptophan metabolism.** *A and B*, TDO KO mice have dramatically elevated levels of brain tryptophan and kynurenine, regardless of LPS treatment (main effect of genotype, tryptophan, $p<0.0001$, ANOVA, kynurenine, $p<0.0001$, ANOVA). *C*, In the brain, the ratio of kynurenine to tryptophan, a measure of flux through the first step of the KP, is lower in TDO KO mice, regardless of LPS treatment (main effect of genotype, $p<0.0001$, ANOVA). *D*, Kynurenine levels in plasma increase in response to LPS in WT and TDO KO mice (main effect of treatment, $p<0.0001$, no interaction, ANOVA). However, TDO KO mice have significantly higher amounts of kynurenine in plasma than WT mice (main effect of genotype, $p=0.0004$, ANOVA). *E*, LPS treatment does not alter brain 5HT levels in WT or TDO KO mice, but TDO KO mice have higher brain 5HT levels (main effect of

genotype, p=0.0233, ANOVA). *F*, TDO KO mice have an increased ratio of 5HIAA to 5HT (main effect of genotype, p<0.0001, ANOVA), implying that these mice have increased 5HT turnover, regardless of LPS treatment. ** p<0.01, *** p<0.001, ANOVA, Bonferroni post test. Points represent mean, and error bars represent SEM.

Figure 6.

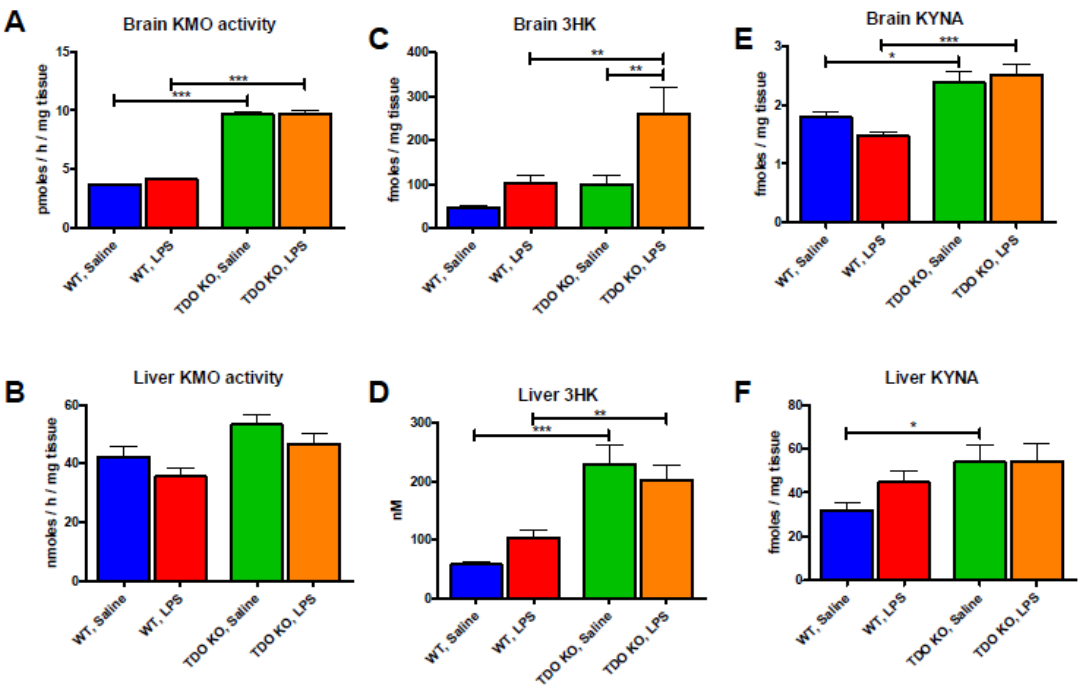

FIGURE 6. **In TDO KO mice, enzyme activity is altered along the 3HK branch of the KP, but metabolite levels are elevated along both branches.** *A,* Brain KMO activity is elevated in TDO KO mice (main effect of genotype, p<0.0001, ANOVA) regardless of LPS treatment. *B*, Liver KMO activity is also elevated in TDO KO mice (main effect of genotype, p=0.0037, ANOVA). *C*, TDO KO mice have significantly higher brain 3HK levels than WT mice (main effect of genotype, p=0.0023), though this is driven primarily by a high level of 3HK in TDO KO mice treated with LPS. However, the LPS-induced increase in brain 3HK levels is not significantly different between TDO KO and WT mice (main effect of treatment, p=0.0017, no interaction, ANOVA). *D*, Liver 3HK levels are higher in TDO KO mice than in WT mice (main effect of genotype, p<0.0001, ANOVA). *E and F*, KYNA levels in brain and liver are significantly higher in TDO

KO mice than in WT mice (main effect of treatment, brain, $p<0.0001$, ANOVA, liver, $p=0.0147$, ANOVA), regardless of LPS treatment. * $p<0.05$, ** $p<0.01$, *** $p<0.001$, ANOVA, Bonferroni post test. Points represent mean, and error bars represent SEM.

Figure 7.

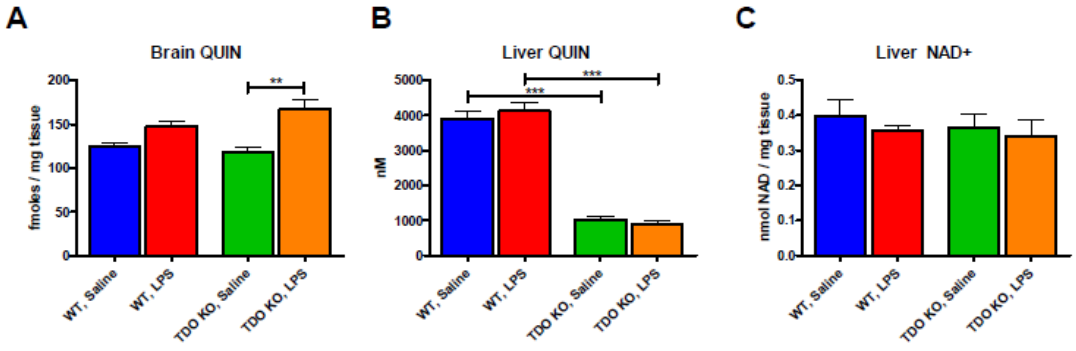

FIGURE 7. **Downstream KP metabolites are altered by LPS and TDO genotype in a tissue-specific manner.** *A*, There is no effect of TDO genotype on brain QUIN levels. *B*, In contrast, liver QUIN levels are dramatically lower in TDO KO mice (main effect of genotype, $p<0.0001$, ANOVA). *C*, Despite this decrease in liver QUIN levels, NAD+ levels in liver are not altered by TDO genotype. ** $p<0.01$, *** $p<0.001$, ANOVA, Bonferroni post test. Points represent mean, and error bars represent SEM.

TABLES

Table 1. Metabolite levels in liver and plasma (IDO cohort)

	WT, saline	WT, LPS	IDO KO, saline	IDO KO, LPS	Effect of LPS?	Effect of genotype?	Interaction?
Liver tryptophan (nM)	58077 +/- 3441	64705 +/- 5096	53505 +/- 2694	60510 +/- 3826	ns	ns	ns
Liver kynurenine (nM)	2595 +/- 201.2	3128 +/- 157	2566 +/- 248.5	2771 +/- 205.3	ns	ns	ns
Liver KYNA (fmoles / mg tissue)	70.03 +/- 7.465	85.97 +/- 10.1	97.93 +/- 28.51	50.5 +/- 5.788	ns	ns	ns
Liver 3HK (nM)	76.1 +/- 5.845	131.1 +/- 13.77	79.7 +/- 6.534	86.6 +/- 8.594	**	*	*
Liver QUIN (nM)	3124 +/- 269.6	2907 +/- 278.2	3284 +/- 226.3	3165 +/- 218.7	ns	ns	ns
Plasma kynurenine (pmoles / mL)	1.83 +/- 0.2955	4.32 +/- 0.611	0.95 +/- 0.1455	1.03 +/- 0.1265	***	***	**
Plasma 3HK (fmoles / mL)	89.83 +/- 13.77	294.4 +/- 47.84	67.95 +/- 7.758	81.21 +/- 4.097	***	***	***
Plasma KYNA (fmoles / mL)	240.5 +/- 48.4	240.4 +/- 25.32	221.5 +/- 30.12	163.2 +/- 15.9	ns	ns	ns

Values are mean +/- SEM. Effect of LPS, effect of genotype and interaction columns refer to main effect as determined by two-factor ANOVA. ns = not significant. * $p<0.05$; ** $p<0.01$; *** $p<0.001$; ANOVA.

Table 2. Enzyme activity in Brain and Liver (IDO cohort)

	WT, Saline	WT, LPS	IDO KO, Saline	IDO KO, LPS	Effect of LPS?	Effect of Genotype?	Interaction?
Brain KMO (pmoles/h/mg tissue)	2.696 +/- 0.0999	2.957 +/- 0.1482	2.752 +/- 0.1029	2.876 +/- 0.05637	ns	ns	ns
Brain KAT I (pmoles/h/mg tissue)	12.66 +/- 0.5486	13 +/- 0.272	13.3 +/- 0.424	13.07 +/- 0.2604	ns	ns	ns
Brain KAT II (pmoles/h/mg tissue)	6.94 +/- 0.2125	7.033 +/- 0.1414	7.244 +/- 0.09876	7.13 +/- 0.215	ns	ns	ns
Brain 3HAO (pmoles/h/mg tissue)	10.34 +/- 0.5519	10.66 +/- 0.4301	9.408 +/- 1.472	9.065 +/- 0.8548	ns	ns	ns
Brain KYNU (fmoles/h/mg tissue)	1146 +/- 125.4	1043 +/- 74.98	990.3 +/- 68.55	1023 +/- 79.75	ns	ns	ns
Liver KMO (nmoles/h/mg tissue)	43.47 +/- 3.518	43.97 +/- 4.74	39.87 +/- 3.161	37.5 +/- 3.598	ns	ns	ns
Liver 3HAO (nmoles/h/mg tissue)	41.76 +/- 0.9424	34.11 +/- 0.7984	40.2 +/- 1.22	34.1 +/- 1.503	****	ns	Ns

Values are mean +/- SEM. Effect of LPS, effect of genotype and interaction columns refer to main effect as determined by two-factor ANOVA. ns = not significant. **** = $p<0.0001$, ANOVA.

Table 3. Metabolite levels in liver and plasma (TDO cohort)							
	WT, saline	**WT, LPS**	**TDO KO, saline**	**TDO KO, LPS**	**Effect of LPS?**	**Effect of genotype?**	**Interaction?**
Liver tryptophan (nM)	51011 +/- 2865	56101 +/- 2670	368039 +/- 16006	297877 +/- 24884	*	***	**
Liver kynurenine (nM)	2245 +/- 222.1	2915 +/- 205.3	12035 +/- 761.3	11095 +/- 388.9	ns	***	ns
Liver KYNA (fmoles / mg tissue)	31.98 +/- 3.594	44.68 +/- 5.369	53.89 +/- 7.628	54.5 +/- 7.743	ns	*	ns
Liver 3HK (nM)	58 +/- 5.369	103.5 +/- 13.45	229 +/- 33.39	202.9 +/- 24.81	ns	***	ns
Liver QUIN (nM)	3898 +/- 221.1	4122 +/- 227	1027 +/- 89.5	885.6 +/- 115.5	ns	***	ns
Plasma kynurenine (pmoles / mL)	1.086 +/- 0.07592	2.287 +/- 0.09339	1.599 +/- 0.1202	3.33 +/- 0.3342	***	***	ns
Plasma 3HK (fmoles / mL)	59.07 +/- 7.284	252.5 +/- 53.55	267.4 +/- 81.21	760.3 +/- 236.6	*	**	ns
Plasma KYNA (fmoles / mL)	96.46 +/- 10.86	143.4 +/- 21.84	122.6 +/- 6.961	173.7 +/- 13.87	**	ns	ns

Values are mean +/- SEM. Effect of LPS, effect of genotype and interaction columns refer to main effect as determined by two-factor ANOVA. ns = not significant. * = $p<0.05$, ** = $p<0.01$, *** = $p<0.001$, ANOVA.

Table 4. Enzyme activity in Brain and Liver (TDO cohort)

	WT, saline	WT, LPS	TDO KO, saline	TDO KO, LPS	Effect of LPS?	Effect of genotype?	Interaction?
Brain KMO (pmoles/h/mg tissue)	3.652 +/- 0.07879	4.116 +/- 0.07936	9.641 +/- 0.2427	9.693 +/- 0.2477	ns	***	ns
Brain KAT I (pmoles/h/mg tissue)	13.73 +/- 0.7578	14.22 +/- 0.7428	13.62 +/- 0.5035	14.11 +/- 0.6536	ns	ns	ns
Brain KAT II (pmoles/h/mg tissue)	7.6 +/- 0.1468	7.96 +/- 0.2377	7.21 +/- 0.2193	7.37 +/- 0.1453	ns	*	ns
Brain 3HAO (pmoles/h/mg tissue)	9.188 +/- 1.273	10.47 +/- 1.036	8.633 +/- 0.8185	9.461 +/- 1.191	ns	ns	ns
Brain KYNU (fmoles/h/mg tissue)	4449 +/- 63.94	4423 +/- 70.33	4402 +/- 128.1	4439 +/- 104.4	ns	ns	ns
Liver KMO (nmoles/h/mg tissue)	42.28 +/- 3.498	35.55 +/- 2.902	53.17 +/- 3.582	46.5 +/- 3.968	ns	**	ns
Liver 3HAO (nmoles/h/mg tissue)	35.6 +/- 0.7299	36.63 +/- 0.9531	35.33 +/- 0.8084	38.31 +/- 0.4561	*	ns	ns

Values are mean +/- SEM. Effect of LPS, effect of genotype and interaction columns refer to main effect as determined by two-factor ANOVA. ns = not significant. * = $p<0.05$, ** = $p<0.01$, *** = $p<0.001$, ANOVA.

Table 5. Summary of KP metabolism in IDO KO and TDO KO mice.

		IDO		TDO	
	Analyte	**Basal effect in KO mice?**	**Is the effect of LPS different in KO?**	**Basal effect in KO mice?**	**Is the effect of LPS different in KO?**
Brain	Tryptophan	ns	no	**increase**	no
	Kynurenine	ns	no	**increase**	no
	Kynurenine / Tryptophan ratio	ns	**yes**	**decrease**	no
	3HK	ns	**yes**	ns	no
	KYNA	ns	**yes**	**increase**	no
	QUIN	ns	**yes**	ns	no
	5HT	ns	no	ns	no
	5HIAA / 5HT ratio	ns	no	**increase**	no
	KMO activity	ns	no	**increase**	no
	3HAO, KYNU, KAT I, KAT II activity	ns	no	ns	no
Liver	Tryptophan	ns	no	**increase**	**yes**
	Kynurenine	ns	no	**increase**	no
	Kynurenine / Tryptophan ratio	ns	no	ns	no
	3HK	ns	**yes**	**increase**	no
	KYNA	ns	no	**increase**	no
	QUIN	ns	no	**decrease**	no
	NAD	ns	no	ns	no
	KMO activity	ns	no	ns	no
	3HAO activity	ns	no	ns	no
Plasma	Kynurenine	ns	**yes**	ns	no
	3HK	ns	**yes**	ns	no
	KYNA	ns	no	ns	no

To evaluate the basal effect of each KO, we compared WT mice treated with saline to KO mice treated with saline using a two-factor ANVOA followed by a Bonferroni post test. To evaluate the effect of LPS in each genotype we used a two-factor ANOVA and concluded that the effect of LPS was different in KO and WT mice when the ANOVA showed a significant interaction ($p<0.05$).

Supplemental Table 1. Primers used for qPCR experiments.

Gene symbol	Gene name	Accession #	Forward Primer	Reverse primer
3-HAO	3-hydroxyanthranilate 3,4-dioxygenase	NM_025325	ctt tca gcc tcc ggt ttg	gcc tcc aac gaa cat gat tt
Afmid	arylformamidase	NM_027827	tca ctt tga cat cat aga gaa tct gac	tct gga aga ctg ttt tca aaa tga
Ahr	aryl hydrocarbon receptor	NM_013464	cgg gtt ccc tgc tca gta	cca gaa gtt caa agc tcc aaa
IDO	indoleamine 2,3-dioxygenase	NM_008324	ggg ctt ctt cct cgt ctc tc	tgg ata cag tgg gga ttg ct
IL-1B	Interleukin 1 beta	NM_008361	ttg acg gac ccc aaa aga t	gaa gct gga tgc tct cat ctg
KMO	kynurenine 3-monooxygenase	NM_133809	tcc ttt caa taa gca gag aaa act ta	ctt cgc att ggc ata gga ct
KYNU	kynureninase	NM_027552	caa acc ctc cca ttt tgt tg	cgc agt cat agt tgc ttg ct
TDO	tryptophan 2,3-dioxygenase	NM_019911	tcc agg gag cac tga tga ta	ctg gaa agg gac ctg gaa tc
Tph2	tryptophan hydroxylase 2	NM_173391	gag ctt gat gcc gac cat	tgg cca cat cca caa aat ac
TNF	tumor necrosis factor alpha	NM_013693	ctg tag ccc acg tcg tag c	ttg aga tcc atg ccg ttg

Supplemental Table 2. Gene expression in brain and liver (IDO cohort)

	WT, saline	WT, LPS	IDO KO, saline	IDO KO, LPS	Effect of LPS?	Effect of genotype?	Interaction?
Brain IDO	1 +/- 0.1089	1.338 +/- 0.1178	--	--	ns (p=0.06)	--	--
Brain TDO	1 +/- 0.06264	0.9268 +/- 0.04414	1.031 +/- 0.06633	0.9462 +/- 0.1189	ns	ns	ns
Brain Afmid	0.9679 +/- 0.03586	1.095 +/- 0.08506	1.055 +/- 0.0446	0.9803 +/- 0.0585	ns	ns	ns
Brain AHR	0.9782 +/- 0.0466	1.07 +/- 0.06796	1.102 +/- 0.05632	0.998 +/- 0.07888	ns	ns	ns
Brain KMO	1 +/- 0.04634	1.27 +/- 0.0814	1.073 +/- 0.04102	1.052 +/- 0.06126	*	ns	*
Brain TPH2	1.188 +/- 0.2814	0.865 +/- 0.08095	1.486 +/- 0.3337	1.308 +/- 0.3516	ns	ns	ns
Brain 3HAO	1.096 +/- 0.05569	1.137 +/- 0.05619	1.15 +/- 0.04071	1.154 +/- 0.1435	ns	ns	ns
Brain IL-1B	1 +/- 0.1947	5.31 +/- 0.759	0.9205 +/- 0.1555	4.768 +/- 0.8038	****	ns	ns
Brain TNF	1 +/- 0.1738	3.515 +/- 0.4066	1.196 +/- 0.08411	3.598 +/- 0.3236	****	ns	ns
Liver 3HAO	1 +/- 0.1238	0.6851 +/- 0.1479	0.9655 +/- 0.1292	0.5796 +/- 0.03989	**	ns	ns
Liver KMO	1 +/- 0.1276	1.159 +/- 0.09765	1.192 +/- 0.1361	1.155 +/- 0.1414	ns	ns	ns
Liver KYNU	1 +/- 0.1058	0.6307 +/- 0.09623	1.133 +/- 0.1496	0.5705 +/- 0.09114	***	ns	ns
Liver TDO	1 +/- 0.1546	0.7173 +/- 0.1795	1.229 +/- 0.2652	0.7462 +/- 0.07979	ns	ns	ns

All units are relative gene expression, normalized to the mean of WT mice treated with saline. Values are mean +/- SEM. Effect of LPS, effect of genotype and interaction columns refer to main effect as determined by two-factor ANOVA,

except for IDO expression, where a t test was used instead of ANOVA. ns = not significant. * $p<0.05$; ** $p<0.01$; *** $p<0.001$; ANOVA.

Supplemental Table 3. Gene expression in brain and liver (TDO cohort)

	WT, saline	WT, LPS	TDO KO, saline	TDO KO, LPS	Effect of LPS?	Effect of genotype?	Interaction?
Brain IDO	1 +/- 0.05671	0.9925 +/- 0.0492	0.8647 +/- 0.04886	1.055 +/- 0.05604	ns	ns	ns
Brain TDO	1 +/- 0.04761	0.9033 +/- 0.03655	--	--	ns	--	--
Brain 3HAO	1 +/- 0.0738	0.9731 +/- 0.06706	1.143 +/- 0.07704	1.098 +/- 0.09003	ns	ns	ns
Brain IL-1B	1 +/- 0.05274	4.666 +/- 0.7357	1.137 +/- 0.07985	4.039 +/- 0.9296	****	ns	ns
Brain KMO	1 +/- 0.0907	1.065 +/- 0.06864	0.8843 +/- 0.05621	0.9758 +/- 0.05531	ns	ns	ns
Brain TPH2	1 +/- 0.1992	0.7778 +/- 0.1432	1.284 +/- 0.4499	1.554 +/- 0.344	ns	ns	ns
Liver KMO	1 +/- 0.08646	1.128 +/- 0.05467	0.9062 +/- 0.065	1.243 +/- 0.1638	*	ns	ns
Liver 3HAO	1 +/- 0.1608	0.4941 +/- 0.0742	0.8331 +/- 0.05232	0.8603 +/- 0.223	ns	ns	ns
Liver KYNU	1 +/- 0.09879	0.6609 +/- 0.05389	0.8864 +/- 0.07481	0.8272 +/- 0.115	*	ns	ns

All units are relative gene expression, normalized to the mean of WT mice treated with saline. Values are mean +/- SEM. Effect of LPS, effect of genotype and interaction columns refer to main effect as determined by two-factor ANOVA, except for TDO expression, where a t test was used instead of ANOVA. ns = not significant. * $p<0.05$; ** $p<0.01$; *** $p<0.001$; ANOVA.

Chapter 4

Conclusions and Future Directions

Summary of results

In this thesis I explored two enzymatic cascades that are induced by immune system activation and that are hypothesized to contribute to neurodegeneration during HD. In Chapter 2, I presented my experiments examining the role of complement component C3 in a mouse model of HD. I found that genetic lack of this complement protein did not alter disease progression, but I also found that this model of disease did not replicate the complement upregulation that is seen in HD patients. These results emphasize the limits of animal models of disease, and provide guidance for future studies of complement in neurodegeneration. In Chapter 3 I investigated how two different enzymes contribute to basal and immune induced Kynurenine Pathway activity. My results obtained using mice lacking tryptophan 2,3-dioxygenase (TDO) indicate that there are previously unappreciated mechanisms that contribute to basal Kynurenine Pathway activity and that experiments using TDO deficient mice will facilitate the identification of these mechanisms. My results obtained using mice lacking indoleamine 2,3-dioxygenase (IDO) indicate that IDO deficient mice are a useful tool for specifically blocking the increase in Kynurenine Pathway activity that occurs after an acute inflammatory challenge such as a lipopolysaccharide (LPS) injection. Interestingly, these LPS induced changes are

reminiscent of the Kynurenine Pathway changes that are seen during neurodegeneration. This raises the possibility that IDO deficiency could block toxic Kynurenine Pathway changes during neurodegeneration, and it will be very important for future experiments to evaluate this hypothesis.

The Discussion sections in Chapters 2 and 3 have already addressed many of the direct implications of my experiments. Thus, in Chapter 4 I will confine my comments to broader questions related to these pathways and their link to neurodegeneration.

Complement in Huntington's Disease

Though complement upregulation is not a feature of the R6/2 mouse model of HD, it is possible that other models of HD do replicate this feature of the disease and thus would provide more insight into the role of complement in HD patients. Alternatively, various complement proteins are upregulated in mouse models of different neurodegenerative disorders, and experiments in those models may lead to more general conclusions on the role of complement in neurodegeneration. Thus, therapies initially targeted at complement in other disorders may ultimately be relevant for HD patients. For example, axotomy of spinal motoneurons leads to both upregulation of complement and loss of synaptic terminals, but C3 deficiency prevents some this synaptic loss [1]. Similarly, complement upregulation occurs in animal models of glaucoma, and pharmacological complement depletion results in amelioration of several disease related phenotypes [2]. These and similar results may teach us enough about the

role of complement during neurodegeneration that future experiments should pursue therapeutic complement manipulation in HD despite the lack of effect that we have shown in one specific mouse model of HD.

It's also important to note that genetic C3 deficiency may have quite different effects than acute pharmacological complement manipulations. Though many experiments have shown that C3 deficient mice have phenotypes consistent with a functional loss of C3 throughout adulthood, there is evidence that other mechanisms can fulfill some of the roles of the complement cascade in the absence of normal C3 expression [3,4]. Pharmacological manipulations are less likely to be impacted by developmental compensatory changes, and there is also an opportunity for pharmacological manipulations to target distinct elements of the complement cascade more specifically. For example, the C3 deficient mice I used lack a crucial complement cascade protein that contributes to both the effector and signaling mechanisms of the complement cascade. However, pharmacological manipulation could attempt to target just one of these functions of C3. Use of a C3aR antagonist would prevent the signaling functions of C3 while permitting the effector functions. In this way, further studies of complement could illuminate circumscribed pieces of the cascade that should be manipulated independently to separate possible beneficial and detrimental functions of the complement cascade.

Kynurenine Pathway therapeutics

The Kynurenine Pathway is important in many diseases, including Huntington's Disease, Alzheimer's Disease, schizophrenia, Multiple Sclerosis and cancer. To date, therapeutics targeting the Kynurenine Pathway have been developed most extensively as cancer treatments. In the local microenvironment of a tumor, it appears that targeting either IDO or TDO would be beneficial. However, my experiments suggest that systemic inhibition of IDO would have very different effects than systemic inhibition of TDO. In either case, systemic dosing of an inhibitor will likely impact brain levels of Kynurenine Pathway metabolites, so drug development efforts need to be aware of possible side effects that impact brain health (namely neurodegeneration and schizophrenia). My results also illustrate that the Kynurenine Pathway is regulated in a tissue and metabolite specific manner. Thus there is no single measurement that will provide a complete picture of Kynurenine Pathway metabolism throughout the body when testing Kynurenine Pathway therapeutics.

The role of inflammation is also of crucial importance in future studies of the Kynurenine Pathway. For example, in naïve conditions inhibition of TDO may strongly modulate kynurenine production, but during inflammation the impact of TDO inhibitors would likely be blunted by increased IDO activity. Further, different inflammatory stimuli may modulate the Kynurenine Pathway differently. Future experiments are necessary to evaluate whether or not chronic inflammatory conditions, such as neurodegenerative disease, employ IDO for Kynurenine Pathway upregulation in the same way as acute inflammatory stimuli, such as an LPS injection. Also, despite the importance of IDO and TDO as rate-

limiting enzymes of the Kynurenine Pathway, the fact that the pathway branches downstream of these enzymes provides an opportunity for further regulation of the pathway. My studies have shown that acute inflammation biases flux of kynurenine through the two branches of the pathway and further experiments will be needed to elucidate the responsible mechanisms. This also highlights the need to investigate the specific Kynurenine Pathway alterations that occur in different disease states as the effects of a given manipulation are likely to vary depending on state of the different mechanisms that regulate the Kynurenine Pathway.

Inflammation and neurodegenerative disease

Connections between inflammation and neurodegenerative disease have been garnering increased attention over the last several years. However, exciting early studies have given way to a more nuanced view of how inflammation may impact neurodegeneration. Some of the first studies on the subject used epidemiological evidence to suggest that non-steroidal anti-inflammatory drugs (NSAIDs) may protect against Alzheimer's Disease [5]. Unfortunately, the prospective clinical trials that followed did not bear out the initial hope that NSAID treatment would provide therapeutic benefit for Alzheimer's patients [6–9]. Instead, focus has shifted towards early, preventative treatment for Alzheimer's Disease – where anti-inflammatory treatments still show some promise – and towards identifying specific aspects of inflammation that are either beneficial or detrimental during neurodegeneration [10]. Similarly, experiments that attempt to

show a causal link between inflammation and neurodegeneration by increasing inflammation and then measuring degeneration have also had mixed results. Studies in mouse models of prion disease [11], Parkinson's Disease [12,13] and Alzheimer's Disease [14] have shown that bouts of peripheral inflammation induced by LPS injections can exacerbate disease progression in some cases. On the other hand, a thorough examination of HD model mice receiving serial LPS injections revealed no exacerbation of disease in these mice [15].

While modulation of inflammation has not yet provided a magic bullet for controlling neurodegeneration, inflammation remains a particularly appealing therapeutic target because inflammatory responses, unlike most neuronal processes, can be altered by drugs that don't cross the blood brain barrier. Several recent studies have shown that this approach can be successful in a variety of disease models. In HD, peripherally restricted drugs that target either cannabinoid signaling or interleukin-6 (IL-6) signaling can alter several readouts of disease progression [16]. In a mouse model of amyotrophic lateral sclerosis, another recent study has shown that manipulating T cell activation outside of the brain can significantly alter disease progression [17]. Also, though it may not be considered typical neurodegeneration, peripheral factors appear to mediate at least some of the decline in cognitive function that is associated with aging [18]. Specifically related to this thesis, a drug that does not cross the blood brain barrier can impact Kynurenine Pathway activity and ameliorate disease progression in a mouse model of HD [19].

These and other studies continue to provide hope that targeting the immune system can help meet the vast unmet need for disease modifying therapeutics in neurodegeneration. In addition to furnishing therapeutic targets, studies of the connection between inflammation and neurodegeneration could improve health by identifying risk factors, aiding in early detection and serving as biomarkers of disease. In order for these efforts to succeed, work such as that outlined in this thesis must continue to elucidate the role of specific aspects of the immune response. Although there is now much evidence illustrating a connection between neurodegeneration and inflammation, we are only just beginning to understand the importance of that connection and how to exploit it for therapeutic benefit.

References

[1] Berg A, Zelano J, Stephan A, Thams S, Barres BA, Pekny M, Pekna M, Cullheim S. Reduced removal of synaptic terminals from axotomized spinal motoneurons in the absence of complement C3. Exp. Neurol. 2012;237(1):8–17.

[2] Jha P, Banda H, Tytarenko R, Bora PS, Bora NS. Complement mediated apoptosis leads to the loss of retinal ganglion cells in animal model of glaucoma. Mol. Immunol. 2011;48(15-16):2151–8.

[3] Huber-Lang M, Sarma JV, Zetoune FS, Rittirsch D, Neff TA, McGuire SR, Lambris JD, Warner RL, Flierl MA, Hoesel LM, Gebhard F, Younger JG, Drouin SM, Wetsel RA, Ward PA. Generation of C5a in the absence of C3: a new complement activation pathway. Nat Med. 2006;12(6):682–7.

[4] Stevens B, Allen NJ, Vazquez LE, Howell GR, Christopherson KS, Nouri N, Micheva KD, Mehalow AK, Huberman AD, Stafford B, Sher A, Litke AM, Lambris JD, Smith SJ, John SWM, Barres BA. The classical complement cascade mediates CNS synapse elimination. Cell. 2007;131(6):1164–78.

[5] McGeer PL, Schulzer M, McGeer EG. Arthritis and anti-inflammatory agents as possible protective factors for Alzheimer's disease: a review of 17 epidemiologic studies. Neurology. 1996;47(2):425–32.

[6] Aisen PS, Davis KL, Berg JD, Schafer K, Campbell K, Thomas RG, Weiner MF, Farlow MR, Sano M, Grundman M, Thal LJ. A randomized controlled trial of prednisone in Alzheimer's disease. Alzheimer's Disease Cooperative Study. Neurology. 2000;54(3):588–93.

[7] Aisen PS, Schafer KA, Grundman M, Pfeiffer E, Sano M, Davis KL, Farlow MR, Jin S, Thomas RG, Thal LJ. Effects of rofecoxib or naproxen vs placebo on Alzheimer disease progression: a randomized controlled trial. JAMA. 2003;289(21):2819–26.

[8] Van Gool WA, Weinstein HC, Scheltens P, Walstra GJ, Scheltens PK. Effect of hydroxychloroquine on progression of dementia in early Alzheimer's disease: an 18-month randomised, double-blind, placebo-controlled study. Lancet. 2001;358(9280):455–60.

[9] Reines SA, Block GA, Morris JC, Liu G, Nessly ML, Lines CR, Norman BA, Baranak CC. Rofecoxib: no effect on Alzheimer's disease in a 1-year, randomized, blinded, controlled study. Neurology. 2004;62(1):66–71.

[10] Van Gool WA, Aisen PS, Eikelenboom P. Anti-inflammatory therapy in Alzheimer's disease: is hope still alive? J. Neurol. 2003;250(7):788–92.

[11] Cunningham C, Campion S, Lunnon K, Murray CL, Woods JFC, Deacon RMJ, Rawlins JNP, Perry VH. Systemic inflammation induces acute behavioral and cognitive changes and accelerates neurodegenerative disease. Biol. Psychiatry. 2009;65(4):304–12.

[12] Pott Godoy MC, Tarelli R, Ferrari CC, Sarchi MI, Pitossi FJ. Central and systemic IL-1 exacerbates neurodegeneration and motor symptoms in a model of Parkinson's disease. Brain. 2008;131(Pt 7):1880–94.

[13] Frank-Cannon TC, Tran T, Ruhn KA, Martinez TN, Hong J, Marvin M, Hartley M, Treviño I, O'Brien DE, Casey B, Goldberg MS, Tansey MG. Parkin deficiency increases vulnerability to inflammation-related nigral degeneration. J. Neurosci. 2008;28(43):10825–34.

[14] Nguyen MD, D'Aigle T, Gowing G, Julien J-P, Rivest S. Exacerbation of motor neuron disease by chronic stimulation of innate immunity in a mouse model of amyotrophic lateral sclerosis. J. Neurosci. 2004;24(6):1340–9.

[15] Franciosi S, Ryu JK, Shim Y, Hill A, Connolly C, Hayden MR, McLarnon JG, Leavitt BR. Age-dependent neurovascular abnormalities and altered microglial morphology in the YAC128 mouse model of Huntington disease. Neurobiol. Dis. 2012;45(1):438–49.

[16] Bouchard J, et al. Journal of Neuroscience. *in press*.

[17] Lincecum JM, Vieira FG, Wang MZ, Thompson K, De Zutter GS, Kidd J, Moreno A, Sanchez R, Carrion IJ, Levine BA, Al-Nakhala BM, Sullivan SM, Gill A, Perrin S. From transcriptome analysis to therapeutic anti-CD40L treatment in the SOD1 model of amyotrophic lateral sclerosis. Nat. Genet. 2010;42(5):392–9.

[18] Villeda SA, Luo J, Mosher KI, Zou B, Britschgi M, Bieri G, Stan TM, Fainberg N, Ding Z, Eggel A, Lucin KM, Czirr E, Park J-S, Couillard-Després S, Aigner L, Li G, Peskind ER, Kaye JA, Quinn JF, Galasko DR, Xie XS, Rando TA, Wyss-Coray T. The ageing systemic milieu negatively regulates neurogenesis and cognitive function. Nature. 2011;477(7362):90–4.

[19] Zwilling D, Huang S-Y, Sathyasaikumar KV, Notarangelo FM, Guidetti P, Wu H-Q, Lee J, Truong J, Andrews-Zwilling Y, Hsieh EW, Louie JY, Wu T, Scearce-Levie K, Patrick C, Adame A, Giorgini F, Moussaoui S, Laue G, Rassoulpour A, Flik G, Huang Y, Muchowski JM, Masliah E, Schwarcz R, Muchowski PJ. Kynurenine 3-monooxygenase inhibition in blood ameliorates neurodegeneration. Cell. 2011;145(6):863–74.

Publishing Agreement

It is the policy of the University to encourage the distribution of all theses, dissertations, and manuscripts. Copies of all UCSF theses, dissertations, and manuscripts will be routed to the library via the Graduate Division. The library will make all theses, dissertations, and manuscripts accessible to the public and will preserve these to the best of their abilities, in perpetuity.

I hereby grant permission to the Graduate Division of the University of California, San Francisco to release copies of my thesis, dissertation, or manuscript to the Campus Library to provide access and preservation, in whole or in part, in perpetuity.

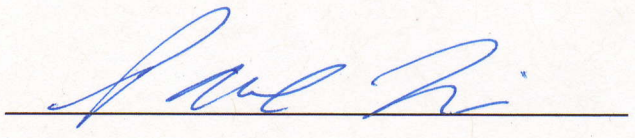

Author Signature

12/18/2012

Date

(This page must be signed and dated by the author and include the correct pagination – as the last numbered page number of your document.)